Generation of primary and secondary gravitational waves in the early universe

A project report
submitted in partial fulfillment for the award of the degree of
Master of Science
in
Physics
by

Tamal Mukherjee

under the guidance of
Dr. L. Sriramkumar

Department of Physics
Indian Institute of Technology Madras
Chennai 600036, India

May 2022

CERTIFICATE

This is to certify that the project titled **Generation of primary and secondary gravitational waves in the early universe** is a bona fide record of work done by **Tamal Mukherjee** towards the partial fulfillment of the requirements of the Master of Science degree in Physics at the Indian Institute of Technology, Madras, Chennai 600036, India.

(L. Sriramkumar, Project supervisor)

ACKNOWLEDGEMENTS

Firstly, I would like to thank IIT Madras for giving us this great opportunity to work on a year-long project. I am thankful to **Dr. L. Sriramkumar** for his guidance, encouragements, motivation and giving me mental support during the tough COVID situation. Without his support, it wouldn't have been possible to complete the project. I would also like to thank Dr. Shiv Sethi for valuable discussions on cosmological perturbations. I would also like to thank Suvashis Maity, Sagarika Tripathy and Saurav Mishra for continuous support and precious discussions. I am also grateful to my parents for always encouraging and supporting me to successfully complete my M.Sc. thesis.

ABSTRACT

The inflationary paradigm is the most promising scenario to generate perturbations in the early universe. A strong prediction of inflation is the generation of primordial gravitational waves (GWs). Over the past few years, the study of the primordial GWs has become a popular interest among the astrophysicists and cosmologists. Direct detection of such GWs background can open a new window to the physics of the very early universe. This project is aimed to understand the generation and evolution primordial GWs. In this report, we have studied the generation of primary GWs from first order tensor perturbations during inflation and their evolution during later epochs. We have found that primary GWs spectrum generated in the $\alpha-$attractor model of inflation can indeed be detected by forthcoming GWs observatories. Apart from these, secondary GWs of detectable amplitudes can also be generated due to the second order scalar-induced tensor perturbations. Considering an ultra-slow-roll model of inflation, we have concluded that the spectrum of secondary GWs can also be detected by some future GWs observatories.

Contents

Chapter 1

Introduction

Gravitational waves (GWs) are plane waves created from the disturbances in the curvature of spacetime, mainly generated by the accelerated masses. These plane waves propagate at the speed of light. GWs were detected (first direct detection) by the LIGO/Virgo collaboration in 2015 [1]. In the past few years, the detections of GWs from binary black hole mergers by LIGO [2] have encouraged the community to come up with experimental proposals to observe GWs over a wide frequency range. It has also sparked an interest to detect GWs of primordial origin. The proposed ground-based and space-based GWs observatories are advanced LIGO (10–10^3 Hz) [3], Einstein Telescope (ET) (1–10^4 Hz) [4]-[5], the Big Bang Observer (BBO) (10^{-3}–10 Hz) [6]-[8], the Deci-hertz Interferometer Gravitational wave Observatory (DECIGO) (10^{-3}–1 Hz) [9]-[11], the Laser Interferometer Space Antenna (LISA) (10^{-5}–1 Hz) [12]-[14], and Square Kilometer Array (SKA) (10^{-9}–10^{-6} Hz) [15].

1.1 Astrophysical versus primordial

There are different sources and types of GWs. Fig. 1.1 illustrates some typical amplitudes and wavelengths of different GWs sources and the sensitivities of some observational probes of GWs (see ref. [16]). While the green portions describe different sources, the violet and red curves are some ongoing and future observational probes of GWs respectively. Different sources and types of GWs can be classified as follows:

1. GWs from binary mergers [17]: Black Hole Binaries (BHB), Neutron Star Binaries (NSB), Super-Massive Black Hole Binaries (SMBHB), White Dwarf Binaries (WDB) , Extreme-Mass-

Ratio Inspirals (EMRI) etc.

2. GWs from spinning Neutron Star (NS): These are known as continuous GWs.

3. Stochastic background of GWs [18]: Apart from these sources mentioned above, there are stochastic backgrounds of GWs, which can be created by large number of independent sources. Astronomers presume that these GWs are passing by all the time and we can get stochastic signals from every direction. A stochastic signal arise from thousands of binary systems which are continuously emitting GWs (at long wavelengths, i.e. $> 10^{14}$ m) in overlapping frequency bands.

It is also believed that another stochastic signal may originate from the very early universe. These relic background of GWs with cosmological origin are known as primordial GWs [19].

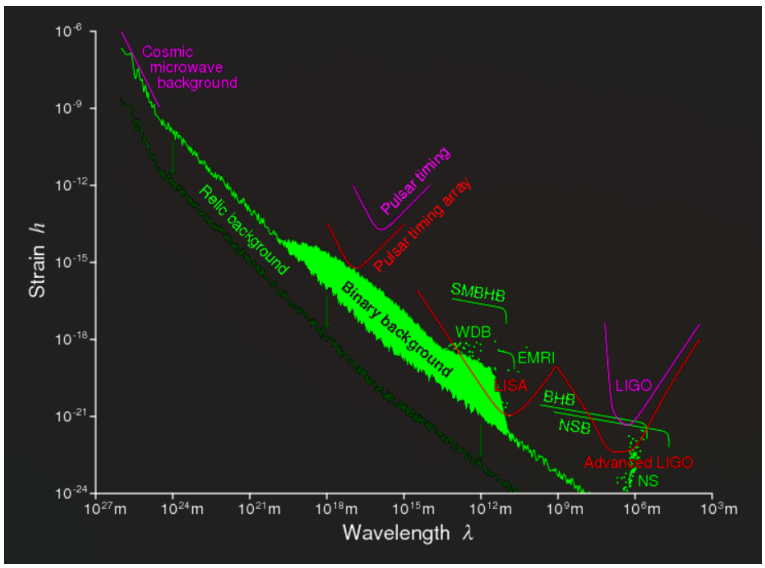

Figure 1.1 : Characteristic strain vs wavelength plot for different GWs sources and observational probes (figure from [17]).

1.2 GWs: probe of the early universe?

Electromagnetic (EM) radiation, neutrinos and GWs are used to study universe. Among them, GWs are the best to probe the very early universe. One and only reason is the weakness of gravity. Since gravity is the weakest fundamental force, GWs decouple immediately upon production and propagate freely (without being reflected, absorbed and refracted) , giving us a clear view of the very early universe. As we know, if the particle interacts very

weekly, then it drops out of thermal equilibrium at a very high energy scale. Therefore, GWs can carry unique information about their origin and the state of the universe at very early epochs and very high energy scales which are unreachable by any other means.

There are studies in the literature about the specific high-energy processes (quantum fluctuations during inflation, particle production [20] during reheating, phase transition [21] and cosmic defects) in the early universe which can generate GWs and determine specific properties of the shape of GWs spectrum. In this work, we have considered the generation of GWs due to the quantum fluctuations during inflation.

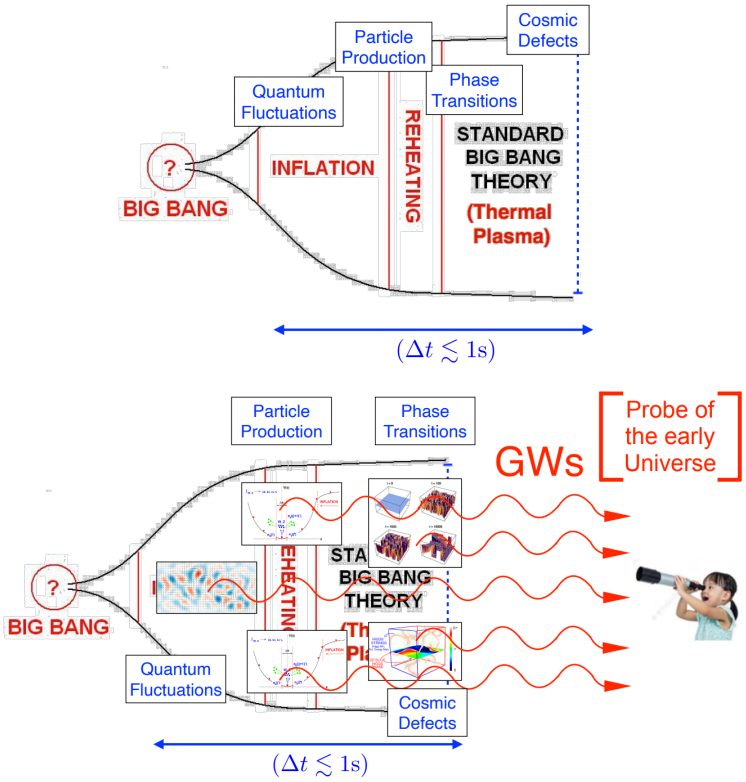

Figure 1.2: GWs from the early universe. [1]

The inflationary scenario offers the most attractive mechanism for the generation of the primordial perturbations which can indeed lead to the formation of primordial GWs. The tensor perturbations generated due to the quantum vacuum fluctuations, are amplified during inflation, which then evolve through the subsequent epochs of the universe before reaching the GW detectors today. Therefore, primordial GWs spectrum today carrys the in-

[1]Figure is taken from Dr. Daniel Figueroa's lecture slides from a lecture given at ICTS Bangalore

formation about their origin as well as evolutionary dynamics.

1.3 A brief outline of the report

In Inflationary scenario, Inflation is assumed to be driven by scalar fields (known as inflaton). In high energy physics, we often deal with scalar field models. Scalar fields can easily achieve the necessary condition that leads to accelerated expansion of the universe. It is also studied that after inflation ends, the universe is reheated through the decay of the inflaton into radiation (known as epoch of reheating), which leads to the beginning of radiation-dominated epoch.

Understanding of the various epoch of the Universe are considerably improved by cosmological observations over past the years [22]-[24]. But due to the lack of direct observations, we don't have any complete information about such an epoch of reheating. The effects of reheating on the dynamics of GWs have already been studied In some standard cosmological scenario (see, Refs. [25]-[27]) and in certain non-standard scenarios (see, for example, Refs. [28]-[30]), the impacts the reheating epoch on the spectrum of GWs have already been studied. In this project, we shall examine the generation of primary GWs from first order tensor perturbation and shall study the impacts of reheating on the spectrum of GWs over different scales. In this project, we have considered two reheating scenarios: i) reheating described by an averaged equation of state (EoS) parameter ω_ϕ, in which case transition from inflaton to radiation happens instantaneously, ii) perturbative reheating, in which case the transition happens gradually through the perturbative decay of inflaton. Finally, we shall analyse our results with the recent GWs observations by the North American Nanohertz Observatory for Gravitational Waves (NANOGrav) [31]. We shall also briefly discuss the secondary phase of reheating and shall explicitly show that the GWs spectrum arises in this scenario can account for the recent NANOGrav observations.

Now, at the second order, tensor perturbations are sourced by first order scalar perturbations. On small scales, an enhancement in the amplitude of the scalar power spectrum can generate secondary GWs when these modes reenter the Hubble radius during radiation dominated epoch. The secondary GWs can also be detected by ongoing and forthcoming GWs observatories like LIGO/Virgo, Pulsar Timing Arrays (PTA) [32]-[33], LISA, BBO, DE-

CIGO and ET.

1.4 Organization of the report:

This thesis is organized as follows. In chapter 2, we shall discuss the motivation for inflation and cosmological perturbation theory and the generation of primary gravitational waves from tensor perturbation. In chapter 3, we shall briefly talk about the epoch of reheating. In chapter 4, we shall discuss the evolution of tensor perturbations during the reheating and radiation dominated epochs. We shall also evaluate the dimensionless energy density of primary GWs today considering the instantaneous reheating scenario. In chapter 5, we shall consider a typical model of inflation and plot the spectrum of primary GWs. We shall also discuss the observational constraints from the forthcoming GWs observatories. We shall discuss the generation of secondary gravitational waves from scalar induced secondary tensor perturbations in chapter 6 and also evaluate the spectrum of secondary GWs today in an ultra-slow-roll model of inflation. We shall explicitly show that spectrum of secondary GWs generated in this model can be detected by future GWs observations. Finally, we shall conclude with a summary of our results. We shall also add two appendices for related derivations.

Notations and conventions:

In this report, we shall work with natural units $\hbar = c = 1$, and shall define the reduced Planck mass $M_{\rm Pl} = (8\,\pi\,G)^{-1/2}$. We shall work in $(3+1)$-spacetime dimensions and use the metric with signature $(-,+,+,+)$. The overdot implies derivative with respect to cosmic time (t) and the overprime implies derivative with respect to conformal time (η). The Greek indices (run from 0 to 3) denote spacetime coordinates and the Latin indices (run from 1 to 3) denote spatial coordinates.

Chapter 2

Generation of primary GWs

The hot big-bang model is the existing theory about the origin and the evolution of our universe. The model describes the expansion of the universe from an initial state of high temperature and density. It can explains a wide range of observed phenomena like light elements abundance, the cosmic microwave background (CMB) radiation , and Hubble-expansion. But there are few shortcomings of the hot Big-Bang model. The inflationary scenario provides a graceful resolution to the shortcomings of the hot Big-Bang model, such as the horizon problem and flatness problem ([34]-[36]). Inflation is a period of accelerated expansion of the universe. Besides solving the mentioned problems, it also provides an mechanism to generate initial seeds of all observed structures in the Universe and CMB anisotropies. We can develope a perturbation theory using the theory of General Relativity, which indeed leads to the density perturbation in the Universe. Apart from that, it also generates tensor perturbations which can describe GWs . We begin this chapter with a summary of the hot Big Bang model, Inflationary paradigm and cosmological perturbation theory. Then we move towards considering quantum aspects of first order tensor perturbations, and explicitly show how the generation of primary GWs.

2.1 Hot big bang cosmology

The basic picture of big bang cosmology describes a hot, dense expanding universe which cools down at late times. This is a very successful model and the success lies on the three significant observations. The first among these is obviously the expansion of the universe. It was discovered that most of the galaxies outside our own Milky Way were continuously

receding from us. Moreover, the velocities of these galaxies turn out to be proportional to their distances. This is well approximated by Hubble's law. In a homogeneous, isotropic expanding universe, at (d $\lesssim 50$ MPc),

$$v_H = H_0 d \tag{2.1}$$

where H_0 is the Hubble constant which determines the present expansion rate of the universe, v_H is the local "Hubble flow" velocity of a source, and d is the proper distance to the source. The best current estimate of the Hubble constant from the Planck measurements of the CMB anisotropies is $H_0 = (67.4 \pm 0.5)$ km s^{-1} Mpc^{-1}.[37]

The second most important observation is the existence of an exceedingly isotropic (to about one part in 10^5) background radiation of relic photons, known as the CMB radiation. The CMB has an almost perfect black body spectrum, and it has a temperature of 2.725 K today [38]. As the energy density of radiation falls faster than matter with the expansion of the universe, the above two observations suggest that the universe was radiation dominated at early times.

Another significant observation which supports the hot big-bang model is the primordial abundances of the light elements which are compatible with the predictions from the theory of big-bang nucleosynthesis (BBN) (see, for instance, Ref. [39] [40]). The abundances of all the light elements depend on the ratio of the number density of baryons to the photons in the universe which does not change with time. Thus the value of this ratio allows us to determine the density of baryon at a given epoch.

2.1.1 The FLRW line element

From observations, we can infer that the universe is homogeneous and isotropic on large scales ($\sim 100 Mpc$) [41]-[44]. The general relativistic description of a homogeneous and isotropic universe is described by the Friedmann-Lemaitre-Robertson-Walker (FLRW) line element, and is given by

$$ds^2 = -dt^2 + a(t)^2 \left[\frac{dr^2}{1 - Kr^2} + r^2 \left(d\theta^2 + sin^2\theta d\phi^2 \right) \right] \tag{2.2}$$

where $a(t)$ denotes the scale factor and t is the cosmic time. The K represents the constant spatial curvature. The universe is spatially flat if $K = 0$, closed if $K > 0$, and open if $K < 0$.

So, K describes the spatial geometry. Apart from the cosmic time, we shall use another time variable known as the conformal time η:

$$\eta = \int \frac{dt}{a(t)} \tag{2.3}$$

Let $\rho(t)$ and $p(t)$ denote the time dependent energy density and the pressure of a matter field or a perfect fluid that is driving the expansion of the universe. The stress-energy tensor of such a perfect fluid is given by

$$T^{\mu}_{\nu} = (\rho + p)u^{\mu}u_{\nu} + p\delta^{\mu}_{\nu} = diag(-\rho, p, p, p) \tag{2.4}$$

where

$$u^{\mu} = (1, 0, 0, 0)$$

is the four-velocity of the fluid described in a comoving coordinate system. Then, the Einstein's equations ($G_{\mu\nu} = \frac{8\pi G}{c^4}T_{\mu\nu}$) corresponding to the Friedmann line element lead to the following two Friedmann equations describing the evolution of the scale factor $a(t)$:

$$H^2 = \left(\frac{8\pi G}{3}\right)\rho - \frac{K}{a^2} \tag{2.5}$$

$$\frac{\ddot{a}}{a} = -\frac{4\pi G}{3}(\rho + 3p) \tag{2.6}$$

where $H = \dot{a}/a$ is the Hubble parameter which indicates the rate of expansion of the universe at any epoch. Now, from the conservation of stress-energy tensor ($\nabla_{\mu}T^{\mu\nu} = 0$), we can arrive at the following time evolution equation for the energy density of the matter field or fluid:

$$\dot{\rho} + 3H(\rho + p) = 0 \tag{2.7}$$

Another key assumption of the the standard cosmology is that the pressure of the matter content of the universe, described by a perfect fluid is directly proportional to the energy density

$$p = w\rho \tag{2.8}$$

where w is the equation of state. Using equation (2.8) and integrating equation (2.6) we get the following relation,

$$\rho(t) \propto a(t)^{-3(1+w)} \tag{2.9}$$

Table: FLRW solutions for the flat universe dominated by radiation, matter or cosmological constant (Λ) ([45]):

Model Universe	w	$\rho(a)$	$a(t)$	$a(\eta)$
Radiation Dominated	$\frac{1}{3}$	a^{-4}	$t^{1/2}$	η
Matter Dominated	0	a^{-3}	$t^{2/3}$	η^2
Λ Dominated	-1	a^0	e^{Ht}	$-\eta^{-1}$

We can see that the energy density of radiation falls faster than that of matter with the expansion of the universe. This immediately points to the fact that the universe has expanded from a hot and dense early radiation dominated phase. From now on-wards, we shall restrict ourselves to the spatially flat ($K = 0$) universe.

2.1.2 Shortcomings of the model

Apart from these remarkable success of the hot big bang model, it has some serious shortcomings too. It is unable to provide a satisfactory explanation to a few cosmological problems like horizon problem, flatness problem, relic density problem, entropy problem etc. We shall discuss only the horizon and flatness problem in this section because these two are arguably the most significant.

1. Horizon Problem:

The horizon problem is the problem of determining the statistical homogeneity and isotropy of the universe on large scales. In other words, why is the temperature of the CMB seen in the opposite directions of the sky almost the same? In the standard hot big bang cosmology, assuming that the universe was radiation dominated all the way from the time of big bang until decoupling, these opposite directions in the sky would have been much larger than the Hubble radius, say, $d_H = H^{-1} = (\dot{a}/a)^{-1}$ at the time of decoupling. Therefore, these antipodal points would not have been in causal contact before this epoch and, hence, there is no way to establish thermal equilibrium over such a length scale. On the other hand, observations indicate that the CMB has roughly the same temperature in different directions of the sky. The horizon problem is, therefore, the lack of an explanation as to why such a large number of (about 10^6) causally disconnected volumes had nearly the same temperature at the time of decoupling.

The horizon is defined as the physical radial distance travelled by a light ray from the big bang at $t = 0$ up to a given time t. It describes the size of the causally connected regions. The horizon size is given by [46]:

$$h(t) = a(t) \int_0^t \frac{d\tilde{t}}{a(\tilde{t})} \tag{2.10}$$

If one assumes the universe to be dominated by non-relativistic matter from the epoch of decoupling t_{dec} until today t_0, and dominated by radiation form $0 < t < t_{dec}$, then the linear dimensions of the backward and forward light cones denoted by l_B and l_F respectively are given by

$$l_B(t_0, t_{dec}) = a_{dec} \int_{t_{dec}}^{t_0} \frac{d\tilde{t}}{a(\tilde{t})} \simeq 3(t_{dec}^2 t_0)^{1/3} \tag{2.11}$$

and,

$$l_F(t_{dec}, 0) = a_{dec} \int_0^{t_{dec}} \frac{d\tilde{t}}{a(\tilde{t})} = 2t_{dec} \tag{2.12}$$

where a_{dec} denotes the value of the scale factor at the epoch of decoupling and we have used the observational fact that $t_0 (\simeq 10^{10}$ years$) \gg t_{dec} (\simeq 10^5$ years) [47].

Then we can find the ratio of the linear dimensions of the backward and the forward light cones at decoupling to be [47]

$$R \equiv \frac{l_B}{l_F} = \frac{3}{2} \left(\frac{t_0}{t_{dec}} \right)^{1/3} \simeq 70 \tag{2.13}$$

From the above equation, we can conclude that at the epoch of decoupling, the linear dimension of the backward light cone is about 70 times larger than the forward light cone. But, it turns out that the CMB is almost isotropic inspite of having no causal connections before decoupling. This is knows as horizon problem. We can state the horizon problem in a different way(as shown in fig. 2.1), in terms of the evolution of the physical wavelength associated with the perturbation.

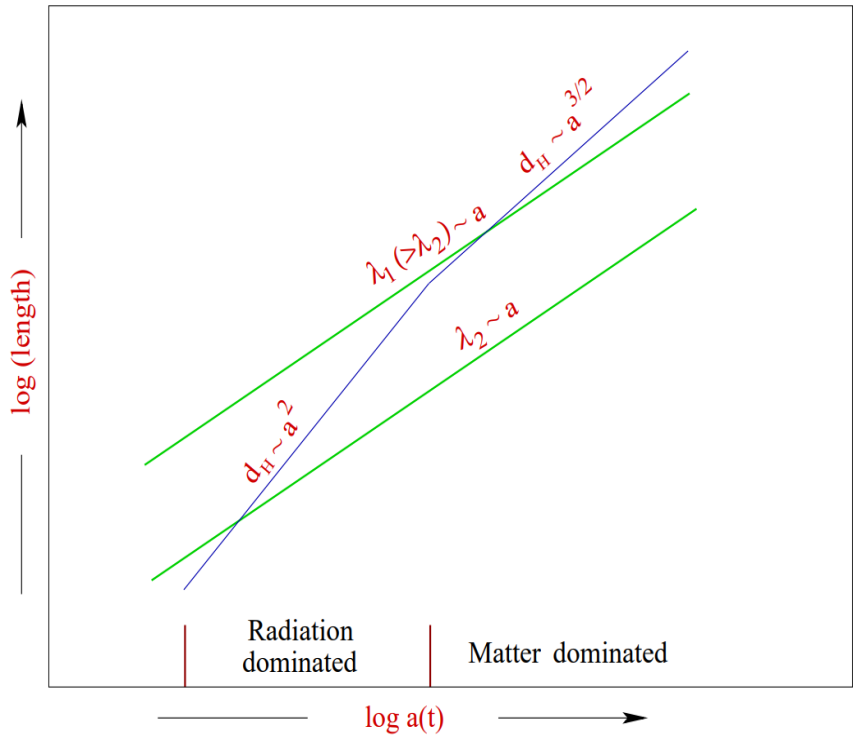

Figure 2.1 : The physical length scales λ_1 and λ_2 ($\lambda_P = a/k$) and the Hubble radius d_H are plotted as a function of the scale factor a on a log log plot during the radiation and the matter dominated epochs. In the standard hot big bang cosmology, all the modes are outside the Hubble radius and, hence, there was no causal contact at very early times. However, the temperature of the CMB is almost the same in different directions, even in the anti-podal points. (Figure from [47])

2. Flatness Problem:

Another drawback of the standard hot big bang model is the flatness problem. It is also referred as cosmological fine-tuning problem. The Friedmann equation viz. Eq. (2.5) can be rewritten as

$$\Omega - 1 = \frac{K}{a^2 H^2} \tag{2.14}$$

where the density parameter Ω is defined as

$$\Omega \equiv \frac{\rho}{\rho_c} \quad \text{with} \quad \rho_c \equiv \frac{3H^2}{8\pi G} \tag{2.15}$$

We can read from the equation (2.14) that $\Omega = 1$ at all the times if the universe is perfectly flat ($K = 0$). Again, the time dependence of $(\Omega - 1)$ will be quite different in the presence of a small curvature term. During radiation dominated epoch, we have $H^2 \propto \rho_r \propto a^{-4}$ and

$$\Omega - 1 \propto \frac{1}{a^2 a^{-4}} \propto a^2 \tag{2.16}$$

During matter dominated epoch, we have $H^2 \propto \rho_m \propto a^{-3}$ and

$$\Omega - 1 \propto \frac{1}{a^2 a^{-3}} \propto a \tag{2.17}$$

So, in the standard big-bang cosmology, $(\Omega - 1)$ decreases when we go backwards with time in both epochs. This means that Ω tends to evolve away from unity with the expansion of the universe. However, since present observations suggest that Ω is within a few percent of unity today (See, for instance [48]), Ω is forced to be much closer to unity in the past.

For example, we can deduce the value of $(\Omega - 1)$ at t_{Pl} (the time at which the temperature of the universe is $T_{Pl} \sim 10^{19} GeV$),

$$\frac{|\Omega - 1|_{T=T_{Pl}}}{|\Omega - 1|_{T=T_0}} \approx \frac{a_{Pl}^2}{a_0^2} \approx \frac{T_0^2}{T_{Pl}^2} \approx \mathcal{O}(10^{-64}) \tag{2.18}$$

where $T_0 \sim 10^{-13}$ GeV is the temperature of the CMB radiation today and a_0 is the scale factor today.

During epoch of nucleosynthesis when light elements were formed, at $T_N \sim 1$ MeV, we get [49]

$$\frac{|\Omega - 1|_{T=T_N}}{|\Omega - 1|_{T=T_0}} \approx \frac{a_N^2}{a_0^2} \approx \frac{T_0^2}{T_N^2} \approx \mathcal{O}(10^{-16}) \tag{2.19}$$

Thus, in order to get an accurate value of $(\Omega_0 - 1) \sim 1$ at present epoch, the value of $(\Omega - 1)$ at early epochs have to be fine-tuned to values close to zero. These initial conditions except these extremely fine tuned ones will eventually lead to either a closed universe that recollapses soon, or to an open universe that quickly enters the curvature dominated regime. This is known as flatness problem.

2.2 Inflationary paradigm

As we discussed above, the hot big-bang model had some serious shortcomings. Almost four decades ago, it was realized that a phase of an accelerated expansion of the universe at very early times can indeed provide a solution to the various problems of the standard hot big bang cosmology. Such a period of an extremely rapid accelerated expansion of the universe is known as "Inflation" which proposed by Alan Guth in 1980 [50].

The length scales of cosmological interest today (say, $1 \lesssim \lambda_0 \lesssim 10^4 Mpc$), were outside the Hubble radius at earlier times prior to their reentry during radiation or matter

domination. These length scales should be inside the Hubble radius (i.e.$\lambda_P < d_H$) in the early times to ensure causal connections which are indeed responsible for the origin of inhomogeneities. Thus, we consider an inflationary epoch in the early universe during which these length scales decreases faster than the Hubble radius [51] , i.e.

$$-\frac{d}{dt}\left(\frac{\lambda_P}{d_H}\right) < 0 \tag{2.20}$$

This definition translates to an equivalent condition that the scale factor of the universe is accelerating during inflation:

$$\ddot{a} > 0 \tag{2.21}$$

In Fig. 2.2, the physical wavelength of two different modes and the Hubble radius have been plotted as a function of the scale factor during inflation and the radiation dominated epochs [47]. In plotting the figure, we have assumed that the inflationary phase is described by a power law expansion of the form $a \propto t^q$ where $q > 1$. Considering this, we can find that $\lambda_P \propto a$ during all the epochs and the Hubble radius d_H behaves as $\frac{1}{q}$ and a^2 during inflation and the radiation dominated epochs respectively. The evolution of physical length scales in this plot gives straight lines with unit slope. The slopes of the straight lines describing the inflationary and the radiation dominated epochs will be

$$\text{During INFLATION: } log(d_H) = \frac{1}{q} log(a) \implies \text{Slope} \ll 1 \text{ when } q \gg 1 \tag{2.22}$$

$$\text{During radiation domination: } log(d_H) = 2log(a) \implies \text{Slope} = 2 \tag{2.23}$$

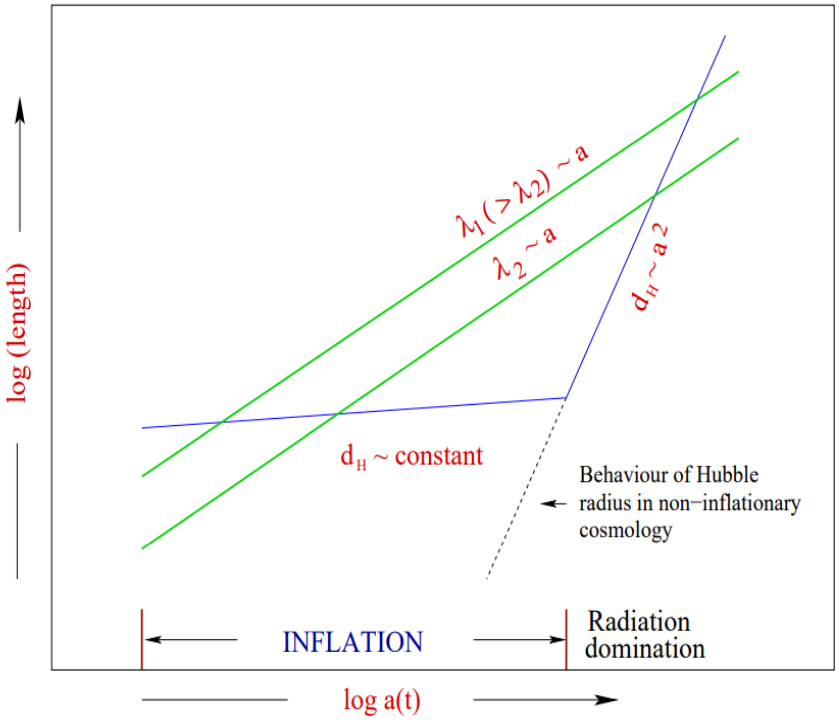

Figure 2.2: : Evolution of the physical length scales (in green) and the Hubble radius (in blue) are plotted as a function of the scale factor $a(t)$ on a log-log plot during the inflation and the radiation dominated epochs (Figure from [47])

It is then clear from the above figure that, inflation is needed in order to bring all the modes inside the Hubble radius and thus making causal connections.

2.2.1 Solution to the horizon problem

To solve the horizon problem, the forward light cone must be at least as large as the backward light cone. For simplicity, we assume that the universe undergoes exponential inflation, say, from time t_i to t_f, during the early stages of the radiation dominated epoch. A period of the universe during which $p = -\rho$ is called the de Sitter universe [52]. In a de Sitter universe,

$$\rho = \text{Constant} \quad \text{and} \quad H_I = \text{Constant} \tag{2.24}$$

where H_I is the constant Hubble parameter during inflation. So we have

$$a = a_0 e^{H_I (t_f - t_i)} \tag{2.25}$$

Let, A denotes the factor by which the scale factor increases during the inflation. In such a case, the size of the horizon at decoupling due to de Sitter inflation is,

$$l_I(t_{dec},0) = a_{dec}\int_0^{t_{dec}} \frac{d\tilde{t}}{a(\tilde{t})} \simeq \left(\frac{a_{dec}}{H_I}\right)\left(\frac{t_{dec}}{t_f}\right)^{1/2} A \tag{2.26}$$

where we have set $t_i = H_I^{-1}$. In such a case, if we choose $H_I \simeq 10^{13}$ GeV, then the ratio of the forward and the backward lightcones at the epoch of decoupling is given by [47]

$$R_I = \frac{l_I}{l_B} \simeq \frac{A}{10^{26}} \tag{2.27}$$

We can clearly see that $R_I = 1$ if $A \simeq 10^{26}$.

The amount of expansion from an initial time t_i to a time t is generally expressed in terms of the number of e-folds defined as follows:

$$N = \int_{t_i}^{t} dt H_I = ln\left[\frac{a(t)}{a_i}\right] \tag{2.28}$$

Thus, we have

$$N = lnA = ln\left(\frac{a_f}{a_i}\right) \simeq 60 \tag{2.29}$$

where a_f is the scale factor at the end of inflation. Thus, we require at least 60 e-folds ($N \gtrsim 60$) to overcome the horizon problem.

2.2.2 Solution to the flatness problem

Inflation also elegantly solves the flatness problem. As the Hubble rate is assumed to be constant during inflation, from equation (2.14), we can see that

$$\Omega - 1 \propto \frac{1}{a^2} \tag{2.30}$$

On the other end, the condition (2.18) suggests that to get a value of $(\Omega_0 - 1)$ of order of unity today, its value at the beginning of the radiation dominated phase must be $|\Omega - 1| \sim 10^{-60}$. Now, in the standard hot big-bang cosmology, the beginning of the radiation dominated phase can be identified with the end of the inflation.

In order to solve the flatness problem, we then require

$$|\Omega_f - 1| \lesssim 10^{-60} \tag{2.31}$$

just after the end of inflation. Here, Ω_f is the value of Ω at the end of inflation (i.e. $t = t_f$). We can write the ratio of $(\Omega - 1)$ between the initial and final phases of inflation, which is given by

$$\frac{|\Omega_f - 1|}{|\Omega_i - 1|} \lesssim \left(\frac{a_i}{a_f}\right)^2 = e^{-2N} \tag{2.32}$$

If we assume $|\Omega_i - 1|$ is of the order unity, then the number of e-folds is required to be $N \gtrsim 60$ in order to solve the flatness problem. From Eq. (2.32), we can infer that, if inflation lasts longer than 60 e-folds, the value of Ω_0 will be equal to unity with a higher precision. Therefore, one can say that

$$\text{INFLATION} \implies \Omega_0 \simeq 1 \tag{2.33}$$

2.3 Inflation with scalar fields

In the previous section, we have seen how inflation, or accelerated expansion in the de Sitter approximation, solves the horizon and flatness problems of the standard Big Bang cosmology. However, a question still arises: What is driving this accelerated expansion of the universe ? In order to have an inflationary epoch in the early universe, it turns out that one needs to have a matter source with negative pressure as neither radiation nor matter allow for such a behavior of the scale factor. From the second Friedmann equation (2.6), it is evident that, for accelerated expansion, we require

$$(\rho + 3p) < 0 \tag{2.34}$$

Now one may think off Einstein's cosmological constant Λ (vacuum energy) which has negative pressure, but a universe dominated by Λ remains the same for the infinite future (eternal inflation), and we can never see a radiation-dominated phase. Again, it can be shown that Λ can not induce metric fluctuations (see ref. [47]).

Therefore, we need a different form of energy which can drive inflation. We shall consider a homogeneous canonical single scalar field ϕ (inflaton) to describe the dynamics of the inflation. Inflaton is described by a potential $V(\phi)$. It can be any fundamental scalar field like the Higgs field or any composite field.
The action for the inflation field reads

$$S = \int d^4x\sqrt{-g}\mathcal{L} = \int d^4x\sqrt{-g}\left[-\frac{1}{2}(\partial_\mu\phi\partial^\mu\phi) - V(\phi)\right] \tag{2.35}$$

where ($\sqrt{-g} = a^3$) for FLRW metric. From the Euler-Lagrange equation

$$\frac{1}{\sqrt{-g}}\partial_\mu\left(\sqrt{-g}\frac{\partial\mathcal{L}}{\partial(\partial_\mu\phi)}\right) = \frac{\partial\mathcal{L}}{\partial\phi} \tag{2.36}$$

we obtain the equation of motion for the homogeneous inflaton

$$\ddot{\phi} + 3H\dot{\phi} + V_\phi = 0 \tag{2.37}$$

where $V_\phi = dV/d\phi$. The associated stress-energy tensor for inflaton is given by

$$T^\mu_\nu = \partial^\mu\phi\partial_\nu\phi - \delta^\mu_\nu\mathcal{L} \tag{2.38}$$

The homogeneity and isotropy of the FLRW background imply that the scalar field will be time-dependant only. Hence, the corresponding stress-energy tensor will be diagonal. In such a case, the energy density ρ and the pressure p associated with the scalar field can be obtained as

$$T^0_0 = -\rho = -\left[\frac{\dot{\phi}^2}{2} + V(\phi)\right] \tag{2.39}$$

$$T^i_j = p\delta^i_j = \left[\frac{\dot{\phi}^2}{2} - V(\phi)\right]\delta^i_j \tag{2.40}$$

Using the above expressions, one finds that the condition for inflation, viz. Eq. (2.34) can be written as

$$\dot{\phi}^2 < V(\phi) \tag{2.41}$$

This implies that the inflation can be achieved if the inflaton is potential dominated. We can rewrite the Friedmann equations (2.5) and (2.6) in terms of the energy density and the pressure associated with the inflaton as

$$H^2 = \frac{1}{3M^2_{Pl}}\left[\frac{\dot{\phi}^2}{2} + V(\phi)\right], \tag{2.42}$$

$$\dot{H} = -\left(\frac{1}{2M^2_{Pl}}\right)\dot{\phi}^2 \tag{2.43}$$

2.3.1 Slow roll inflation

The conventional approximation which guarantees inflation is known as the slow roll approximation [53]. Under this approximation, the kinetic energy of the inflaton is neglected as compared to its potential energy when the field rolls slowly down the potential, i.e.

$$\dot{\phi}^2 \ll V(\phi) \tag{2.44}$$

Also, in order to lead to the required amount of inflation, the acceleration term is also ignored when compared to the Hubble friction term in Eq. 2.37.

$$\ddot{\phi} \ll 3H\dot{\phi} \tag{2.45}$$

Hence we require a sufficiently flat potential for the inflaton which ensures slow roll for a sufficiently long time in order to achieve enough inflation. Upon using these two slow-roll conditions, we arrive at the following equations

$$H^2 \simeq \frac{1}{3M_{Pl}^2} V(\phi), \tag{2.46}$$

$$3H\dot{\phi} \simeq V_\phi \tag{2.47}$$

Given a potential $V(\phi)$, we can define two dimensionless parameters describing the slow-roll inflation as [47]:

$$\epsilon_V = \left(\frac{M_{Pl}^2}{2}\right)\left(\frac{V_\phi}{V}\right)^2 \quad \text{and} \quad \eta_V = M_{Pl}^2\left(\frac{V_{\phi\phi}}{V}\right) \tag{2.48}$$

where $V_{\phi\phi} = d^2V/d\phi^2$ and these parameters have to be much smaller than unity. These are known as potential slow- roll parameters. In the slow-roll approximation,

$$\epsilon_V \ll 1 \quad \text{and} \quad \eta_V \ll 1 \tag{2.49}$$

There are another set of parameters known as Hubble slow-roll (HSR) parameters which can be defined in terms of the derivatives of the Hubble parameter. These are defined as follows [47]:

$$\epsilon_H = 2M_{Pl}^2\left(\frac{H_\phi}{H}\right)^2 = -\left(\frac{\dot{H}}{H^2}\right) \tag{2.50}$$

$$\delta_H = 2M_{Pl}^2\left(\frac{H_{\phi\phi}}{H}\right) = \epsilon_H - \left(\frac{\dot{\epsilon_H}}{2H\epsilon_H}\right) \tag{2.51}$$

These parameters satisfy the following conditions:

$$\epsilon_H \ll 1, \quad \delta_H \ll 1, \quad \text{and} \quad \mathcal{O}(\epsilon_H^2, \delta_H^2, \epsilon_H\delta_H) \ll \epsilon_H \tag{2.52}$$

It turns out that the HSR parameters can be a better choice to describe the slow roll approximation (see, Ref. [47]; also see Ref. [53]).

For a given slow-roll parameter ϵ_n, we can define higher order slow-roll parameters as follows:

$$\epsilon_{n+1} = \frac{dln|\epsilon_n|}{dN} \tag{2.53}$$

where N is the number of e folds.

2.3.2 Quadratic potential : background evolution

In this section, we shall consider a quadratic potential and evaluate all the background quantities corresponding to the dynamics of inflation. Let us consider the following quadratic potential :

$$V(\phi) = \frac{1}{2}m^2\phi^2 \tag{2.54}$$

where m is the mass of the inflaton ϕ. Using the first Friedmann equation, Eq.(2.42) in Eq. (2.37), we get

$$\frac{d\dot{\phi}}{d\phi} = -\frac{\sqrt{12\pi G(\dot{\phi}^2 + m^2\phi^2)}\dot{\phi} + m^2\phi}{\dot{\phi}} \tag{2.55}$$

The behaviour of the solution to the above equation is shown in figure 2.4, which shows the attractor solution [54] given by the equation

$$3H\dot{\phi} = -m^2\phi \implies \dot{\phi}_{atr} \approx \pm\frac{m}{\sqrt{12\pi G}} = \pm\frac{mM_{\rm Pl}}{\sqrt{3/2}}$$

Here $(+)$ sign corresponds to $\phi < 0, \dot{\phi} > 0$ and the $(-)$ sign corresponds to $\phi > 0, \dot{\phi} < 0$..

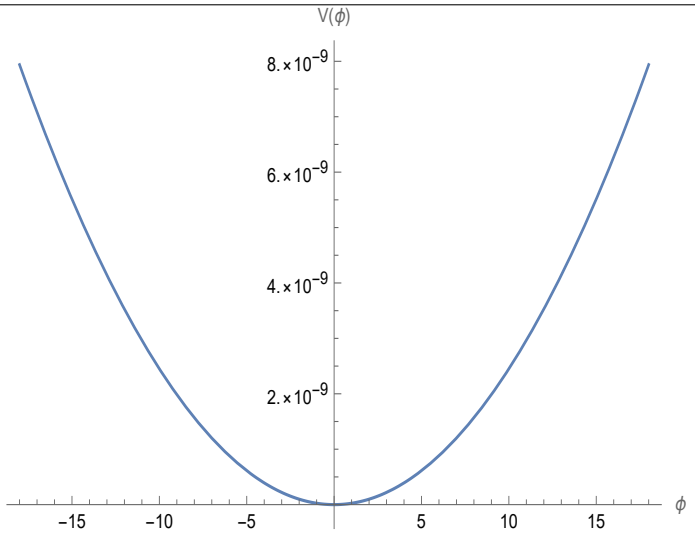

Figure 2.3: Plot of $V(\phi) = \frac{1}{2}m^2\phi^2$ vs ϕ where $m = 7 \times 10^{-6}$

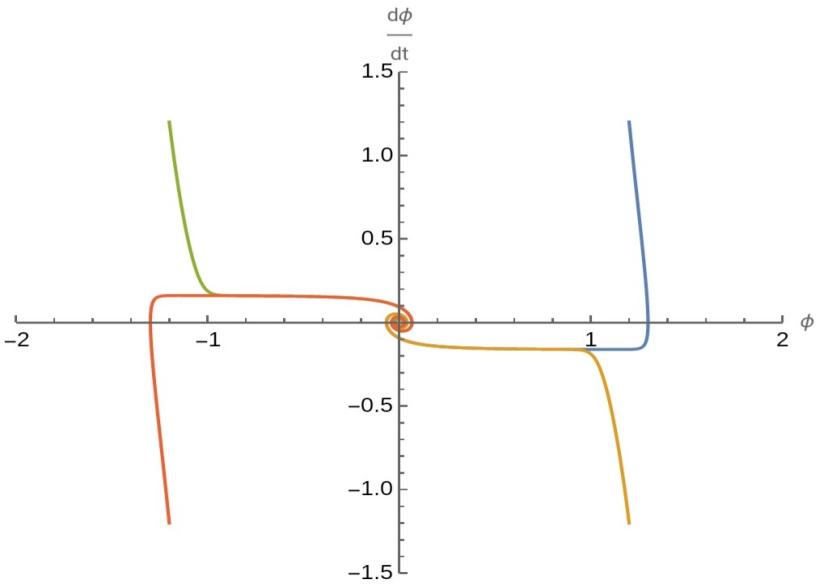

Figure 2.4: The phase space diagram which shows the attractor solutions.

We can easily find that the equation of motion for the inflaton field (see equation (2.37)) can be written in terms of the number of e folds N as

$$\frac{d^2\phi}{dN^2} + \left[3 - \frac{1}{2}\left(\frac{d\phi}{dN}\right)^2\right]\frac{d\phi}{dN} + \left[6 - \left(\frac{d\phi}{dN}\right)^2\right]\frac{1}{2V(\phi)}\frac{dV(\phi)}{d\phi} = 0 \tag{2.56}$$

The Hubble parameter can be written as

$$H(N) = \left[\frac{2V(\phi)}{6 - \left(\frac{d\phi}{dN}\right)^2}\right]^{1/2} \tag{2.57}$$

We can write the first slow-roll parameter ϵ_1 as

$$\epsilon_1(N) = \frac{1}{2}\left(\frac{d\phi}{dN}\right)^2 \tag{2.58}$$

where we have set $M_{Pl} = 1$ for all the equations. We numerically solve the equation (2.56) and plot $\phi(N), H(N)$ and $\epsilon_1(N)$.

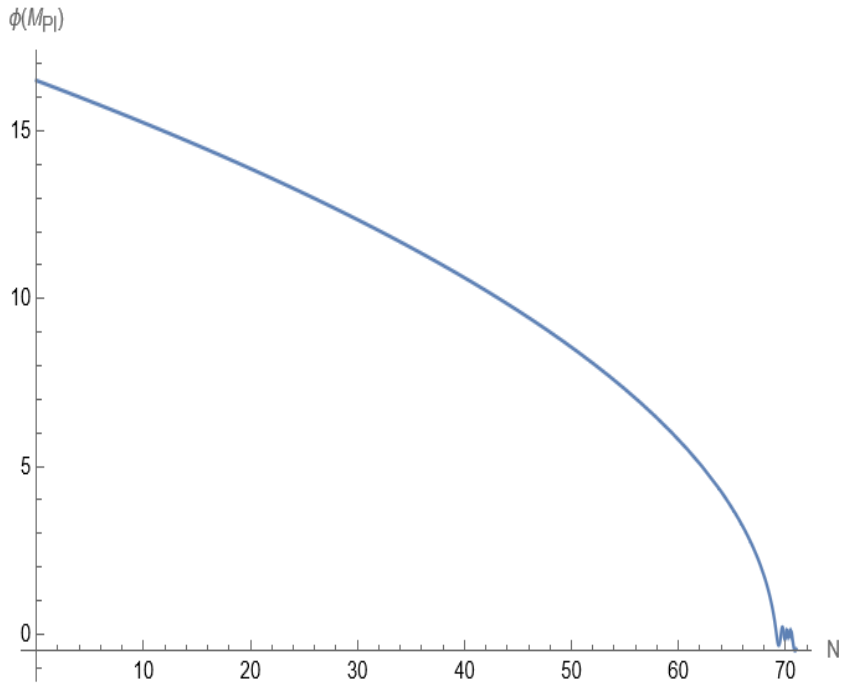

Figure 2.5: Numerical estimate of the scalar field ϕ as a function of N for the quadratic potential.

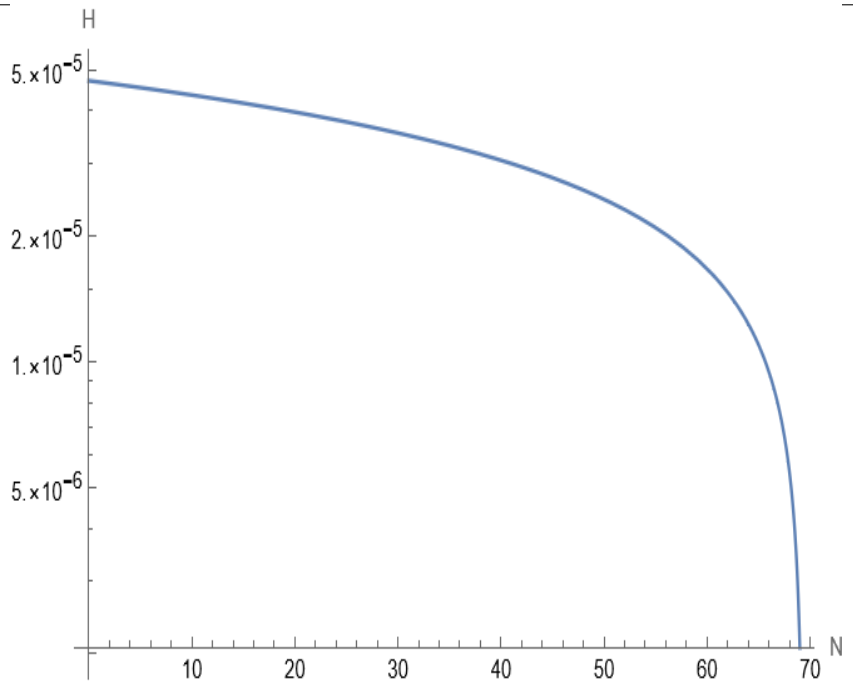

Figure 2.6: Numerical estimate of the Hubble parameter H as a function of N.

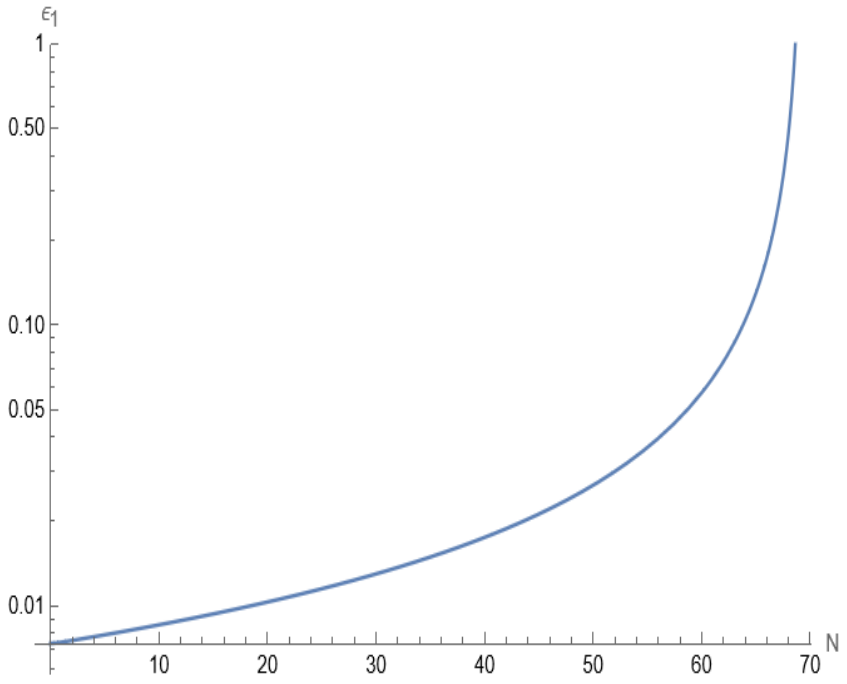

Figure 2.7: Numerical estimate of the first slow-roll parameter ϵ_1 as a function of N for the quadratic potential.

2.4 Linear cosmological perturbation theory

Apart from solving the problems of hot big-bang cosmology, inflation provides a mechanism to generation primordial fluctuations that can evolve and amplified with the expansion of the universe and form the large scale structures observed today ([55], [54], [53]). From CMB observations we know that the anisotropies at the epoch of decoupling are about one part in 10^5 which are very small. So, these were even smaller in earlier epochs. Therefore, we can study the linear perturbation theory until structure-formation. The theory was developed by Lifshitz [56]. Significant progress in the understanding cosmological perturbations was achieved by Bardeen [57], who proposed a gauge-invariant formalism for cosmological perturbation. In this section, we shall briefly describe the generation of primordial perturbations. We shall then discuss the quantization of these perturbations and define power spectra, which can be constrained by observations.

2.4.1 Classifications of perturbations

The theory of cosmological perturbation can be studied upon expanding the Einstein equations to linear order about the background metric. The first step in the analysis is to classify metric fluctuations according to their transformation properties under local spatial rotations on hypersurfaces of constant time. The metric perturbations in the homogeneous FLRW background can be decomposed into scalar, vector and tensor perturbations. In the linear theory, each fluctuation modes evolve independently.

We begin by expanding the metric about the FLRW background $g^{(0}_{\mu\nu}$ [58]

$$g_{\mu\nu} = g^{(0)}_{\mu\nu}(t) + \delta g_{\mu\nu}(\vec{x}, t) \tag{2.59}$$

where $\delta g_{\mu\nu}$ denotes perturbation in the metric tensor. Since the metric is a symmetric tensor, there are $\frac{4(4+1)}{2} = 10$ degrees of freedom in $\delta g_{\mu\nu}$ at first sight.

There are four degrees of freedom associated with the scalar metric fluctuations

$$\delta g^{(scalar)}_{\mu\nu} = a^2(\eta) \begin{bmatrix} -2A & B_{,i} \\ B_{,i} & 2(-\psi\delta_{ij} + E_{,ij}) \end{bmatrix} \tag{2.60}$$

where A, ψ, B and E are four scalar functions describing the scalar perturbation (comma denotes ordinary partial derivative and δ_{ij} is the Kronecker delta.)

There are also four degrees of freedom associated with the vector metric fluctuations,

$$\delta g_{\mu\nu}^{(vector)} = a^2(\eta) \begin{bmatrix} 0 & S_i \\ S_i & -(F_{i,j} + F_{j,i}) \end{bmatrix} \tag{2.61}$$

where S_i and F_i are two divergence-less ($\nabla_i S^i = \nabla_i F^i = 0$) vector functions.

Finally, there are two degrees of freedom corresponding to tensor metric perturbation,

$$\delta g_{\mu\nu}^{(tensor)} = a^2(\eta) \begin{bmatrix} 0 & 0 \\ 0 & h_{ij} \end{bmatrix} \tag{2.62}$$

where $h_{ij} \ll 1$ is a symmetric, transverse ($\nabla_i h^{ij} = 0$) and traceless ($h^i_i = 0$) tensor.

So, we have three types of metric perturbations. Scalar perturbations are responsible for the inhomogeneities and the anisotropies in the universe. In our work, we are interested in the tensor perturbations which describe gravitational waves. Interestingly, GWs can be generated even in the absence of sources [59].

Gauge transformation:

In discussing cosmological perturbations, one has to deal with two spacetimes - the physical, perturbed spacetime and an unperturbed background spacetime, here described by FLRW metric. Points in background spacetime are labelled by coordinates x^μ. A gauge transformation induces a small amplitude transformation in the coordinates of physical spacetime. We can define gauge transformation as

$$x^\mu \to \tilde{x}^\mu = x^\mu + \xi^\mu \tag{2.63}$$

where $\xi^\mu \ll 1$. The componentξ^0) contributes to a scalar metric fluctuation. We can decompose the spatial three-vector ξ^i as follows

$$\xi^i = \xi^i_{tr} + \gamma^{ij}\xi_{,j} \tag{2.64}$$

where γ^{ij} is the spatial background metric, ξ^i_{tr} is the transverse component with two degrees of freedom, which lead to the vector perturbations. The second term (given by gradient of a scalar ξ) capitulate scalar perturbations. To summarize, there are two scalar gauge modes given by ξ_0 and ξ and two vector gauge modes given by the transverse three vector ξ^i_{tr}. There exist no tensor type gauge transformation. Thus, finally there remain two scalar, two vector and two tensor fluctuation modes.

Gauge choices: We often use two approaches to deal with gauge degrees of freedom in the cosmological perturbation theory. The first approach is to pick a gauge, i.e, to pick conditions in the coordinates which completely eliminate gauge freedom. The second is to construct gauge invariant quantities. For our project, we shall work with a fixed-gauge. There are many different gauge choices. Two well-motivated choices for gauges in scalar perturbations are the synchronous gauge and the conformal-Newtonian (longitudinal) gauge.

1. Synchronous gauge: Synchronous gauge is determined by $\delta g_{0\mu} = 0$. They correspond to the gauge choice $A = 0$ and $B = 0$. But, this does not fix the coordinates uniquely (for a detailed discussion, see [54]).

2. Longitudinal (conformal-Newtonian) gauge: Longitudinal gauge is defined by the choices: $B = 0, E = 0$. These conditions fix the coordinate system uniquely [54].

In this report, we shall work in the longitudinal gauge. First, we will consider the **scalar perturbation**. The choice of gauge corresponds to $A = \Phi, \psi = \Psi, B = E = 0$. The Friedmann line element in this gauge is given by [47]

$$ds^2 = -(1 + 2\Phi)dt^2 + a^2(t)(1 - 2\Psi)d\mathbf{x}^2 \tag{2.65}$$

We have two independent scalar degrees of freedom (Φ, Ψ). Neglecting anisotropic stresses, we can obtain the perturbed stress-energy tensor as

$$\delta T^0_0 = -\delta\rho; \quad \delta T^0_i = -\nabla_i \delta\sigma; \quad \delta T^i_j = \delta p \delta^i_j \tag{2.66}$$

where $\delta\rho$, $\delta\sigma$ and δp denote the fluctuations in the energy density, momentum flux, and pressure, respectively. We can then use the above expressions in the perturbed first order Einstein's equations, viz. $\delta G^\mu_\nu = 8\pi G \delta T^\mu_\nu$, we obtain

$$\delta G^0_0 = 6H(\dot{\Phi} + H\Phi) - \frac{2}{a^2}\nabla^2\Phi = -8\pi G\delta\rho \tag{2.67a}$$

$$\delta G^0_i = -2\nabla_i(\dot{\Phi} + H\Phi) = -8\pi G\nabla_i\delta\sigma \tag{2.67b}$$

$$\delta G^i_j = 2[\ddot{\Phi} + 4H\dot{\Phi} + (2\dot{H} + 3H^2\Phi)]\delta^i_j = 8\pi G\delta p\delta^i_j \tag{2.67c}$$

where we have set $\Phi = \Psi$ in the absence of anisotropic stresses.

The amplitude of scalar perturbations Φ, also known as the Bardeen potential [57], is interestingly a gauge-invariant quantity. The Eqs. (2.67a) and (2.67c) can be combined to obtain the equation governing the evolution of the Bardeen potential [54] given by

$$\Phi'' + 3(1+c_s^2)\mathcal{H}\Phi' - c_s^2\nabla^2\Phi + [2\mathcal{H}' + (1+3c_s^2)\mathcal{H}^2]\Phi = 4\pi G a^2 \tau\delta S \tag{2.68}$$

where $\mathcal{H} = \frac{a'}{a}$ is the conformal Hubble parameter, $c_s = \sqrt{\frac{p'}{\rho'}}$ is the adiabatic speed of perturbations and δS is the entropy perturbation which can be written in terms of the non-adiabatic pressure perturbation δp^{NA} as [54]

$$\tau\delta S = \delta p^{NA} \tag{2.69}$$

where τ can be written as $\tau = \frac{c_s^2\rho}{S}$. So we can write total pressure perturbation considering entropy perturbation as

$$\delta p = c_s^2\delta\rho + \tau\delta S \tag{2.70}$$

Let us consider the following gauge-invariant quantity which is a combination of Bardeen known as curvature perturbation defined as [47]

$$\mathcal{R} = \Phi + \left(\frac{2\rho}{3\mathcal{H}}\right)\left(\frac{\Phi' + \mathcal{H}\Phi}{\rho + p}\right) \tag{2.71}$$

This quantity is proportional to the local scalar curvature on the spatial hypersurface. Using equation (2.68), in the fourier space, we have,

$$\mathcal{R}_k' = \left(\frac{\mathcal{H}}{\mathcal{H}^2 - \mathcal{H}'}\right)[4\pi G a^2 \delta p_k^{NA} - c_s^2 k^2 \Phi_k] \tag{2.72}$$

Now, on super-Hubble scales, i.e $\frac{k}{\mathcal{H}} \ll 1$, it can be easily seen that curvature perturbation $\mathcal{R}_k$ remain conserved.

We shall now consider the **vector perturbations**. In this case, the Friedmann line element would be

$$ds^2 = -dt^2 + a^2(t)[\delta_{ij} + (\nabla_i F_j + \nabla_j F_i)]dx^i dx^j \tag{2.73}$$

The perturbed Einstein tensor can be obtained as

$$\delta G_0^0 = 0 \tag{2.74a}$$

$$\delta G_i^0 = -\frac{1}{2}\nabla^2 \dot{F}_i \tag{2.74b}$$

$$\delta G_j^i = \frac{1}{2}\left[3H(\nabla_i \dot{F}_j + \nabla_j \dot{F}_i) + (\nabla_i \ddot{F}_j + \nabla_j \ddot{F}_i)\right] \tag{2.74c}$$

We must have $\delta G_i^0 = 0$ and $\delta G_j^i = 0$ in the absence of source (as in the case of inflation driven by scalar fields). We can see from the above equations that F_i also vanishes in that case. So, there will be no vector perturbations in the absence of sources with vorticity.

Finally, we consider the **tensor perturbations**. In this case, Friedmann line element can be written as

$$ds^2 = a^2(\eta)[-d\eta^2 + (\delta_{ij} + h_{ij}]dx^i dx^j \tag{2.75}$$

where h_{ij} is the symmetric, transverse, traceless 2nd rank tensor which has two degrees of freedom. Tensor perturbations is important for our discussions as we shall see later, these two degrees of freedom of h_{ij} correspond to the two polaizations of gravitational waves. The perturbed Einstein tensor can be obtained as

$$\delta G_0^0 = 0 \tag{2.76a}$$

$$\delta G_i^0 = 0 \tag{2.76b}$$

$$\delta G_j^i = \frac{1}{2}\left(\ddot{h}_{ij} + 3H\dot{h}_{ij} - \frac{1}{a^2}\nabla^2 h_{ij}\right) \tag{2.76c}$$

In the absence of anisotropic stresses, in first order, one can arrive at the following differential equation for tensor perturbation

$$h_{ij}^{''} + 2\mathcal{H}h_{ij}^{'} - \nabla^2 h_{ij} = 0 \tag{2.77}$$

where we have expressed the equation in conformal time coordinate for later use. This differential equation admits non-trivial solutions even in the absence of a source term which implies that, on quantization, tensor perturbations can be generated even in the absence of sources.

2.4.2 Quantization of scalar perturbations and scalar power spectrum

In this section, we shall consider the quantum fluctuations associated with the inflaton, which act as seed of inhomogeneities in the early universe. We can define tiny perturbations in the inflaton $\delta\phi$ as

$$\phi^{(perturbed)} = \phi + \delta\phi \tag{2.78}$$

where ϕ is the homogeneous background inflaton. These tiny fluctuations evolve with the expansion of the universe and leave their imprints as the anisotropies in the CMB. As we know, on super-Hubble scales, curvature perturbations are proportional to Bardeen potential Φ_k, which determines anisotropies in CMB. So, we are interested in the spectrum of curvature perturbations generated during inflation. At the linear order, the components of the perturbed stress-energy tensor associated with the inflaton can be expressed as

$$\delta T^0_0 = -\dot{\phi}\dot{\delta\phi} + \dot{\phi}^2\Phi - V_\phi\delta\phi = -\delta\rho \tag{2.79a}$$

$$\delta T^0_i = -\nabla_i(\dot{\phi}\delta\phi) = -\nabla_i(\delta\sigma) \tag{2.79b}$$

$$\delta T^i_j = (\dot{\phi}\dot{\delta\phi} - \dot{\phi}^2\Phi - V_\phi\delta\phi)\delta^i_j = \delta p\delta^i_j \tag{2.79c}$$

In these equations, we have set $\Phi = \Psi$ as the scalar field does not possess any anisotropic stress. Using the above expressions, we can easily obtain the equation governing the Bardeen potential can be written as

$$\Phi'' + 3(1+c_s^2)\mathcal{H}\Phi' - c_s^2\nabla^2\Phi + [2\mathcal{H}' + (1+3c_s^2)\mathcal{H}^2]\Phi = (1-c_s^2)\nabla^2\Phi \tag{2.80}$$

Upon comparing this equation with equation (2.68), we can express the non-adiabatic component of the pressure perturbation associated with the inflaton as

$$\delta p^{NA} = \left(\frac{1-c_s^2}{4\pi G a^2}\right)\nabla^2\Phi \tag{2.81}$$

As we know that the primordial perturbations are expected to generate from quantum fluctuations, therefore we can write the corresponding quantum operator $\hat{\mathcal{R}}$ of the classical curvature perturbations and can express it in the homogeneous background universe as

$$\hat{\mathcal{R}}(\eta,\mathbf{x}) = \int \frac{d^3\mathbf{k}}{(2\pi)^{3/2}}\left[\hat{a}_\mathbf{k}\mathcal{R}_k(\eta)e^{i\mathbf{k}\cdot\mathbf{x}} + \hat{a}^\dagger_\mathbf{k}\mathcal{R}^*_k(\eta)e^{-i\mathbf{k}\cdot\mathbf{x}}\right] \tag{2.82}$$

where the creation and the annihilation operators $\hat{a}_{\mathbf{k}}$ and $\hat{a}^{\dagger}_{\vec{k}}$ obey the standard commutation relations.

Substituting equation (2.81) in equation (2.72) and differentiating further, we get the differential equation for curvature perturbation in Fourier space

$$\mathcal{R}_k^{''} + 2\left(\frac{z'}{z}\right)\mathcal{R}_k' + k^2\mathcal{R}_k = 0 \tag{2.83}$$

where the "pump field" z is defined as $z = \frac{a\dot{\phi}}{H} = \frac{a\phi'}{\mathcal{H}}$. Now upon using Mukhanov-Sasaki variable ([60]-[61] $v_k = \mathcal{R}_k z$, we can rewrite the above differential equation as

$$v_k^{''} + \left[k^2 - \left(\frac{z''}{z}\right)\right]v_k = 0 \tag{2.84}$$

The power spectrum of the curvature perturbation, i.e. scalar power spectrum, denoted by $\mathcal{P}_S(k)$ is the statistical property of the scalar perturbations which are described by the two-point function of the quantum field $\hat{\mathcal{R}}$. It can be expressed as follows

$$\left\langle 0\middle|\hat{\mathcal{R}}_{\mathbf{k}}(\eta)\hat{\mathcal{R}}_{\mathbf{k}'}(\eta)\middle|0\right\rangle = \frac{(2\pi)^2}{2k^3}\mathcal{P}_S(k)\delta^{(3)}(\mathbf{k}+\mathbf{k}') \tag{2.85}$$

where $|0\rangle$ is the vacuum state, i.e, $\hat{a}_{\mathbf{k}}|0\rangle = 0$ for all $\mathbf{k}$. Using equation (2.82), we get the form of scalar power spectrum as

$$\mathcal{P}_S(k) = \frac{k^3}{2\pi^2}|\mathcal{R}_k|^2 = \frac{k^3}{2\pi^2}\left(\frac{|v_k|}{z}\right)^2 \tag{2.86}$$

We can evaluate the RHS of the above equation on super-Hubble scales when curvature perturbation approaches a constant value. Inflation generally predicts a power law form for $\mathcal{P}_S(k)$, i.e.

$$\mathcal{P}_S(k) \propto k^{(n_s-1)} \tag{2.87}$$

where n_s is the scalar-spectral index, which is an important inflationary parameter that can be constrained by observations. Recent observation suggest that [37] $n_s = 0.9649 \pm 0.0042$.

2.4.3 Quantization of tensor perturbations and GWs

Inflaton does not generate vector perturbations as it is a scalar source. Tensor perturbations, which described GWs, can be generated even in the absence of source. Primordial GWs generated from these tensor perturbations also leave their imprints on CMB [62]. We can

similarly quantize the tensor perturbations as well. On quantization, the tensor perturbations $\hat{h}_{ij}$ can be decomposed in terms of the Fourier modes h_k as follows:

$$\hat{h}_{ij}(\eta, \mathbf{x}) = \int \frac{d^3\mathbf{k}}{(2\pi)^{3/2}} \hat{h}_{ij}^{\mathbf{k}}(\eta) e^{i\mathbf{k}\cdot\mathbf{x}}$$

$$\implies \hat{h}_{ij}(\eta, \vec{x}) = \sum_{\lambda=+,\times} \int \frac{d^3\mathbf{k}}{(2\pi)^{3/2}} \left[\hat{a}_{\mathbf{k}}^{\lambda} \epsilon_{ij}^{\lambda}(\mathbf{k}) h_k(\eta) e^{i\mathbf{k}\cdot\mathbf{x}} + \hat{a}_{\mathbf{k}}^{\lambda\dagger} \epsilon_{ij}^{\lambda *}(\mathbf{k}) h_k^*(\eta) e^{-i\mathbf{k}\cdot\mathbf{x}}\right] \tag{2.88}$$

where ϵ_{ij}^{λ} is the polarization tensor. The index λ denotes the two polarization (i.e. $+, \times$) of the gravitational waves. The polarization tensor obeys the relations $\delta^{ij}\epsilon_{ij}^{\lambda}(\mathbf{k}) = 0$ (traceless) and $k^i \epsilon_{ij}^{\lambda}(\mathbf{k}) = 0$ (transverse), and the normalization condition is $\epsilon^{ij\,\lambda}(\mathbf{k})\epsilon_{ij}^{\lambda'\,*}(\mathbf{k}) = 2\delta^{\lambda\lambda'}$.

In the absence of sources with anisotropic stresses, The Fourier mode h_k satisfies the following differential equation

$$h_k^{''} + 2\frac{a'}{a} h_k^{'} + k^2 h_k = 0 \tag{2.89}$$

where we have considered the anisotropic stress to be zero. We now define the Mukhanov-Sasaki variable for the tensor pertrubations as $u_k = a h_k M_{\rm Pl}/\sqrt{2}$. In terms of this variable, the above equation can be written as

$$u_k^{''} + \left[k^2 - \left(\frac{a''}{a}\right)\right] u_k = 0 \tag{2.90}$$

The tensor power spectrum $\mathcal{P}_T(k)$ can be expressed using the two-point function

$$\left\langle 0 \middle| \hat{h}_{ij}^{\mathbf{k}}(\eta) \hat{h}_{mn}^{\mathbf{k}'}(\eta) \middle| 0 \right\rangle = \frac{(2\pi)^2}{2k^3} \frac{\Pi_{ij,mn}^{\mathbf{k}}}{4} \mathcal{P}_T(k) \delta^{(3)}(\mathbf{k} + \mathbf{k}') \tag{2.91}$$

where $|0\rangle$ is again the vacuum state (i.e. $\hat{a}_{\mathbf{k}}|0\rangle = 0$ for all $\mathbf{k}$ and λ) and

$$\Pi_{ij,mn}^{\mathbf{k}} = \sum_{\lambda} \epsilon_{ij}^{\lambda}(\mathbf{k}) \epsilon_{mn}^{\lambda *}(\mathbf{k}) \tag{2.92}$$

From the above decomposition, we get

$$\mathcal{P}_T(k) = 4\frac{k^3}{2\pi^2}|h_k|^2 = \tag{2.93}$$

Another observable inflationary parameter is the tensor-to-scalar ratio

$$r = \left(\frac{\mathcal{P}_T}{\mathcal{P}_S}\right) \tag{2.94}$$

We do not have any direct observation of primordial tensor power spectra yet. But there is an observational uper bound on the tensor-to-scalar ratio [63] 'r', which is $r < 0.036$. Tensor power spectrum will be nearly scale invariant in the slow roll approximation (see Appendix A),

$$\mathcal{P}_T(k) \simeq \left(\frac{2H^2}{\pi^2 M_{Pl}^2}\right)_{k=aH} \tag{2.95}$$

We shall now assume the de Sitter approximation for slow-roll inflation in which the scale factor in conformal time is given by

$$a(\eta) = \frac{1}{1 - H_I\eta} \tag{2.96}$$

, where H_I is the constant Hubble parameter during inflation, as we discussed before. In such a case, we have

$$\frac{a''}{a} = \frac{2H_I^2}{(1 - H_I\eta)^2} \tag{2.97}$$

In order to solve equation (2.90), which is a second order differential equation, we need initial conditions. The well-motivated initial conditions for primordial perturbations which are available in the literature is known as Bunch-Davies initial conditions on sub-Hubble scales,

$$\lim_{\frac{k}{\mathcal{H}}\to\infty}(u_k(\eta)) \to \frac{1}{\sqrt{2k}}e^{-ik\eta} \tag{2.98}$$

As the modes remain well inside the Huuble-radius (i.e $\frac{k}{\mathcal{H}} \gg 1$), they do not feel the expansion of the universe (do not feel the curvature of spacetime). Thus, solutions to these modes take the Minkowskian form: $e^{\pm ik\eta}$. So, initially, the modes start in the vacuum which requires that u_k are positive-frequency modes on sub-Hubble scales and therefore they have the above asymptotic form (i.e equation (2.98)).

Imposing the Bunch-Davies initial conditions, we have the solution to the equation (2.89), in de Sitter approximation,

$$u_k(\eta) = \frac{1}{\sqrt{2k}}\left[1 + \frac{iH_I a(\eta)}{k}\right]e^{-ik\eta} \tag{2.99}$$

Equivalently, we have

$$h_k(\eta) = \frac{\sqrt{2}}{M_{Pl}}\frac{u_k}{a} = \frac{\sqrt{2}}{M_{Pl}}\frac{1}{\sqrt{2k}}\left[1 + \frac{iH_I a(\eta)}{k}\right]e^{-ik\eta} \tag{2.100}$$

Using the form of scale factor in equation (2.96), we can write

$$h_k(\eta) = h_k(a) = \frac{\sqrt{2}}{M_{Pl}} \frac{iH_I}{\sqrt{2k^3}} \left[1 - \frac{ik}{H_I a(\eta)}\right] e^{-ik/H_I} e^{ik/H_I a(\eta)} \tag{2.101}$$

Let $a_f = a(\eta_f)$, where a_f is the scale factor at the end of the inflation and η_f is the conformal time at the end of inflation such that $0 < \eta_f < H_I^{-1}$. Upon using the above solution, the tensor power spectrum at the end of the inflation can be obtained as

$$\mathcal{P}_T(k) = \frac{2H_I^2}{\pi^2 M_{Pl}^2} \left(1 + \frac{k^2}{k_f^2}\right) \tag{2.102}$$

where $k_f = a_f H_I$ is the mode which leaves the Hubble-radius at the end of the inflation. In the limit $k \ll k_f$, the power spectrum reduces to

$$\mathcal{P}_T(k) \simeq \frac{2H_I^2}{\pi^2 M_{Pl}^2} \tag{2.103}$$

which is scale-invariant and this scale-invariance is valid only for $k \ll k_f$ since the de Sitter form of the scale factor would not hold true near the end of inflation. therefore, we shall mostly restrict ourselves to the modes with wave numbers $k < 10^{-2} k_f$ Though, the tensor power spectrum will contain a small spectral tilt in the slow-roll approximation but we shall ignore this for our discussions. In a later chapter, we shall show how tensor power spectrum can be used to obtain the present day GWs spectrum.

2.5 Dimensionless Energy Density of GWs

In order to obtain the expression for the dimensionless energy density of GWs, we start with the action governing the tensor perturbations. At quadratic order in h_{ij}, tensor perturbations in the absence of anisotropic stress are governed by the action [64]

$$S = \int d^4\mathbf{x}\sqrt{-g}\mathcal{L} = \int d^4\mathbf{x}\sqrt{-g}\left[\frac{-g^{\mu\nu}}{64\pi G}\partial_\mu h_{ij}\partial_\nu h_{ij}\right] \tag{2.104}$$

where $g^{\mu\nu}$ and g is the inverse and determinant of the unperturbed background metric $g_{\mu\nu}$ respectively. We can use this action to compute the stress-energy tensor

$$T_{\alpha\beta} = -2\frac{\delta\mathcal{L}}{\delta g^{\alpha\beta}} + g_{\alpha\beta}\mathcal{L} \tag{2.105}$$

Then, the energy density of GWs at any given time (η) is given by

$$\rho_{GW}(\eta) = -T_0^0 = \frac{M_{Pl}^2}{8a^2}\left(\frac{1}{2}\left\langle \hat{h_{ij}'^2}\right\rangle + \left\langle |\boldsymbol{\nabla}\hat{h}_{ij}|^2\right\rangle\right) \tag{2.106}$$

We can also define energy density per logarithmic interval, say, $\rho_{GW}(k,\eta)$ through the relation

$$\rho_{GW}(k) = \int_0^\infty d\ lnk\ \rho_{GW}(k,\eta) \tag{2.107}$$

Upon using the above equation and equation (2.88), we get $\rho_{GW}(k,\eta)$ to be

$$\rho_{GW}(k,\eta) = \frac{M_{Pl}^2}{2a^2}\frac{k^3}{2\pi^2}\left(|h_k'(\eta)|^2 + k^2|h_k(\eta)|^2\right) \tag{2.108}$$

The observable quantity is the dimensionless energy density $\Omega_{GW}(k,\eta)$, which is defined as

$$\Omega_{GW}(k,\eta) = \frac{\rho_{GW}(k,\eta)}{\rho_c(\eta)} = \frac{\rho_{GW}(k,\eta)}{3H^2M_{Pl}^2} \tag{2.109}$$

where $\rho_c(\eta)$ is the critical energy density as defined in equation (2.15). The quantity of our interest is the present day dimensionless energy density of GWs (i.e. $\Omega_{GW}(k)$). Frequency, f can be written in terms of the wave number k of the tensor modes as

$$f = \frac{k}{2\pi} = 1.55\times10^{-15}\left(\frac{k}{1\ \text{Mpc}^{-1}}\right)\ \text{Hz} \tag{2.110}$$

We shall often refer $\Omega_{GW}(f)$ as the spectrum of GWs today.

Chapter 3

Epoch of Reheating

It is assumed that during inflation, radiation does not interact with scalar field (inflaton). As we had discussed earlier, the factor by which the scale factor increases during the inflationary epoch, i.e $A \simeq 10^{26}$. As the temperature T behaves as inversely proportional to the scale-factor, (i.e. $T \propto 1/a$), the universe cools down rapidly during inflation. In order to rescue the standard hot big-bang scenario after inflation, the universe has to go through an epoch during which the universe must be heated back to the same temperature as it was before inflation. This epoch is known as the epoch of reheating. This process of reheating the universe can be achieved by the coherent oscillation of inflaton about the minimum of the potential followed by the coherent inflaton decays and the transfer of energy from inflaton to radiation ([65]).

3.1 Oscillations of the inflaton

Inflation ends when the field approaches the minimum of the potential and begins to oscillate about it. This is a coherent oscillation, the phase being the same at all points in the large homogeneous region that inflation creates. A typical inflationary potential is shown in the figure 3.1 which shows the oscillation of inflaton about the minimum of the potential.

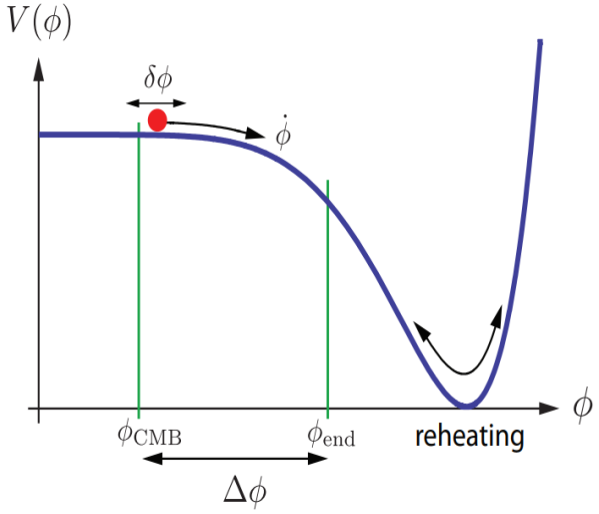

Figure 3.1: A typical example of inflationary potential. Inflaton oscillates about the minimum of the potential during the epoch of reheating (figure from [66]).

This oscillation of inflaton can last for some period if there are no rapid decays of particles. Thus the particle decay time still may be much longer than the Hubble time. This type of situation can be described by looking at the time-averaged behaviour of the inflaton. Upon using the form of energy density and pressure from equation (2.39) and (2.40) and putting these in equation (2.7), we can easily obtain the time evolution equation of the energy density of inflaton as

$$\dot{\rho}_\phi = -3H\dot{\phi}^2 \tag{3.1}$$

which can further be written as

$$\dot{\rho}_\phi = -6H[\rho_\phi - V(\phi)] \tag{3.2}$$

Taking the time average of this equation over a period of oscillation of the inflaton, and making use of the fact that the Hubble parameter remains almost constant over a period of the oscillation, we obtain

$$\langle\dot{\rho}_\phi\rangle = -\langle 6H[\rho_\phi - V(\phi)]\rangle \simeq -6H\langle\rho_\phi - V(\phi)\rangle \tag{3.3}$$

Let ϕ_m be the value of the inflaton when the amplitude of oscillation is maximum. We shall now assume that, over one period,

$$\langle\rho_\phi \simeq V(\phi_m)\rangle = V_m = \text{Constant} \tag{3.4}$$

Considering this, we can easily arrive at the following equation

$$\langle \rho_\phi - V(\phi) \rangle \simeq \bar{\alpha} \langle \rho_\phi \rangle \tag{3.5}$$

where $\bar{\alpha}$ is given by [67]

$$\bar{\alpha} = \left[\int_{-\phi_m}^{\phi_m} d\phi \sqrt{1 - \frac{V(\phi)}{V_m}} \right] \left[\frac{d\phi}{\sqrt{1 - \frac{V(\phi)}{V_m}}} \right]^{-1} \tag{3.6}$$

Thus, we have

$$\langle \dot{\rho}_\phi \rangle = -3H\alpha \langle \rho_\phi \rangle \tag{3.7}$$

where we have set $\alpha = 2\bar{\alpha}$. The above equation can easily be integrated to obtain following expression:

$$\rho_\phi = \rho_0 \left(\frac{a}{a_0} \right)^{-3\alpha} \tag{3.8}$$

Now, in the large-field model (i.e. $V(\phi) \propto \phi^n$), it can be shown that [68], $\alpha = 2n/(n+2)$. Then from the above equation, it can be seen that, in a quadratic potential (i.e. $n = 2$), the average energy density ρ_ϕ of inflaton behaves as nonrelativistic matter. Whereas, for a quartic potential (i.e. $n = 4$), it behaves as radiation.

3.2 Coherent inflaton decays: transferring energy to radiation

We shall now consider multicomponent fluid containing both scalar field (inflaton) and radiation. The decay of inflaton will happen once Hubble time reaches the decay time. In order to achieve the transfer of energy from inflaton to radiation, we need to account for the the interactions between inflaton and radiation too. If we allow the transfer of energy between components, then we can write the the covariant derivative of the stress-energy tensor as follows:

$$\nabla_\mu T^{\mu\nu}_{(\phi)} = Q^\nu_{(\phi)} \quad \text{and} \quad \nabla_\mu T^{\mu\nu}_{(R)} = Q^\nu_{(R)} \tag{3.9}$$

where $Q^\nu_{(\phi)}$ and $Q^\nu_{(R)}$ are four vectors denoting the transfer of energy-momentum from radiation to the inflaton and vice-versa and $T^{\mu\nu}_{(\phi)}$ and $T^{\mu\nu}_{(R)}$ are the stress-energy tensor for inflaton

and radiation respectively. Now from the conservation of the total stress-energy tensor, we can easily see

$$\nabla_\mu[T^{\mu\nu}_{(\phi)} + T^{\mu\nu}_{(R)}] = 0 \quad \Longrightarrow \quad Q^\nu_{(\phi)} + Q^\nu_{(R)} = 0 \tag{3.10}$$

We have denoted ρ_ϕ and p_ϕ as the energy density and pressure of inflation respectively. Denoting ρ_R and p_R as the energy density and pressure of radiation, we have the total energy density and pressure of the two-components system as follows:

$$\rho = \rho_\phi + \rho_R \ \text{ and } \ p = p_\phi + p_R \tag{3.11}$$

The time-component ($\mu = 0$) of the conservation equation (3.10) leads to

$$\dot{\rho}_\phi = -3H(\rho_\phi + p_\phi) + Q_\phi \tag{3.12}$$

$$\dot{\rho}_R = -3H(\rho_R + p_R) + Q_R \tag{3.13}$$

Now, from equation (3.10), we have $Q_\phi = -Q_R$, using this we obtain

$$\dot{\rho} = \dot{\rho}_\phi + \dot{\rho}_R = -3H(\rho + p) \tag{3.14}$$

If we now choose $Q_\phi = -(\Gamma_\phi \dot{\phi}^2)$ where Γ_ϕ is the inflaton-decay rate [68]. For now, we assume Γ_ϕ to be constant. In such a case, the conservation equation (3.12) is given by

$$\dot{\rho}_\phi = -3H(\rho_\phi + p_\phi) - \Gamma_\phi \dot{\phi}^2 = -(3H + \Gamma_\phi)\dot{\phi}^2 \tag{3.15}$$

where we have used $\rho_\phi + p_\phi = \dot{\phi}^2$. Now using equation (2.39), we can further write it as

$$\dot{\rho}_\phi = -2(3H + \Gamma_\phi)[\rho_\phi - V(\phi)] \tag{3.16}$$

Again, using equation (2.39) and writing ρ_ϕ in terms of ϕ and V, we can easily arrive at the following modified equation of motion for inflaton [viz. Eq (2.37)]:

$$\ddot{\phi} + (3H + \Gamma_\phi)\dot{\phi} + V_\phi = 0 \tag{3.17}$$

If we now return to the situation wherein inflaton oscillates about the bottom of the potential, then assuming the interaction between inflaton and radiation, we obtain (from Eq (3.16) the evolution of time averaged density (averaging over oscillations) [viz. Eq (3.3)]:

$$\langle \dot{\rho}_\phi \rangle = -(3H + \Gamma_\phi)\alpha \langle \rho_\phi \rangle \tag{3.18}$$

We can easily integrate the above equation (considering de Sitter approximation) to arrive at the energy density of inflaton

$$\rho_\phi(t) = \rho_0 \left(\frac{a}{a_0}\right)^{-3\alpha} e^{-\Gamma_\phi \alpha (t-t_0)} \tag{3.19}$$

where, t_0 denotes the time at which the inflaton begins to oscillate. This equation essentially implies that the coupling between inflaton and radiation leads to an exponential decay of the inflaton energy density. As we shall see soon, this energy is transferred to radiation, reheating the universe.

We can similarly get the evolution equation for the energy density of radiation as

$$\dot{\rho}_R = -(4H\rho_R + \Gamma_\phi \alpha \rho_\phi) \tag{3.20}$$

where we have used $p_R = \rho_R/3$. On substituting the solution ρ_ϕ [viz. Eqn (3.19)] into this equation and integrating, we get [67]

$$\rho_R(t) = \rho_0(\alpha\Gamma_\phi) \left(\frac{a}{a_0}\right)^{-4} \int_{t_0}^{t} \left[\frac{a(\tilde{t})}{a_0}\right]^{(4-3\alpha)} e^{-[\alpha\Gamma_\phi(\tilde{t}-t_0)]} \tag{3.21}$$

Considering a domain in which the inflaton still dominates the energy density, we get the evolution of the scale factor as

$$\frac{a(t)}{a_0} = (t/t_0)^\beta \tag{3.22}$$

where $\beta = 2/(3\alpha)$. In such case, as $2 \leq n < \infty$, we have $(5/3) \geq (4\beta - 1) > (1/3)$. Then, it can be easily seen [for a detailed discussion, see ref. [67]] that ρ_R first starts to increase. After reaching a maximum value, it starts decreasing.

Chapter 4

Evolution of primary GWs

In the 2nd chapter, we discussed tensor perturbations generated during inflation. We arrived at the tensor power spectrum at the end of the inflation and also showed how the strength or the energy density of GWs are related to the amplitude of tensor perturbations. Now, it is obvious that the dimensionless energy density of GWs observed today ($\Omega_{GW}(k)$) not only depends on the amplitude of the tensor perturbations at the end of the inflation, but also it depends on their evolution through later epochs. In this chapter, we shall discuss the evolution of primary GWs during reheating and radiation dominated epochs and shall finally arrive at the analytical expression for Ω_{GW} today.

4.1 Evolution during reheating

In order to understand the evolution of tensor perturbations after inflation, we shall introduce a quantity known as the tensor transfer function, χ_k. The Fourier amplitude of the tensor perturbations in the post inflationary epochs can be written as [64]

$$h_k(\eta) = h_k^P \chi_k(\eta) \tag{4.1}$$

where h_k^P denotes primordial amplitude tensor perturbations at the end of the inflation. Interestingly, χ_k and h_k obeys same equation of motion. Using equation (2.100), we can write h_k^P as

$$h_k^P = h_k(a_f) = \frac{\sqrt{2}}{M_{Pl}} \frac{iH_I}{\sqrt{2k^3}} \left[1 - \frac{ik}{k_f}\right] e^{-ik/H_I} e^{ik/k_f} \tag{4.2}$$

where $k_f = a_f H_I$ as defined earlier. In this section, we shall discuss the evolution of χ_k during the reheating epoch. From now onwards, we shall work with a re-scaled scale factor

$A = a/a_f$ as the independent variable. It can be found that the evolution equation of transfer function χ_k is given by [69]

$$\frac{d^2\chi_k}{dA^2} + \left(\frac{4}{A} + \frac{1}{H}\frac{dH}{dA}\right)\frac{d\chi_k}{dA} + \frac{(k/k_f)^2}{(H/H_I)^2}\chi_k = 0 \tag{4.3}$$

Note that, the evolution of χ_k depends on the behaviour of Hubble parameter. Now, the goal is to solve the above differential equation for the transfer function during the epoch of reheating. In order to do that, we need initial conditions for χ_k and $d\chi_k/dA$ at the end of the inflation when $A = 1$, i.e. $a = a_f$. Clearly, we have from equation (4.1),

$$\chi_k^I(A = 1) = 1 \tag{4.4}$$

Upon using equation (2.101) and the expression for h_k^P, we can find that

$$\frac{d\chi_k^I(A = 1)}{dA} = -\frac{(k/k_f)^2}{1 - i\left(\frac{k}{k_f}\right)} \simeq 0 \tag{4.5}$$

where the second equality holds only for $k \ll k_f$.

In this section, we shall consider two reheating scenarios:

1. Reheating described by an averaged equation of state parameter (w_ϕ), which is associated with the coherent inflaton oscillations around the minimum of the inflationary potential, as discussed in the previous chapter. In this case, transition from inflaton to radiation happens instantaneously.

2. Perturbative reheating scenario, in which transfer of energy from inflaton to radiation happens gradually.

In the following two sub-sections, we shall discuss the evolution of transfer function in these two scenarios.

4.1.1 Instantaneous reheating

In this sub-section, we shall consider the epoch of reheating described by an averaged equation of state (EoS) parameter, w_ϕ. In such a case, energy density of inflation behaves as [viz. Eq (2.9)], $\rho_\phi \propto a^{-3(1+w_\phi)}$. Then the Hubble parameter can be written as

$$H^2 = H_I^2 A^{-3(1+w_\phi)} \tag{4.6}$$

Thus, we have

$$\frac{1}{H}\frac{dH}{dA} = -\frac{3}{2}(1+w_\phi)\frac{1}{A} \tag{4.7}$$

Upon using these two equations in equation (4.3), the evolution equation for transfer function becomes

$$\frac{d^2\chi_k}{dA^2} + (5-3w_\phi)\frac{1}{2A}\frac{d\chi_k}{dA} + \frac{(k/k_f)^2}{A^{(1-3w_\phi)}}\chi_k = 0 \tag{4.8}$$

The general solution to this differential equation can be expressed in terms of Bessel functions as follows:

$$\chi_k^{RH}(A) = A^{-\nu}\left[C_k J_{-\nu/\gamma}\left(\frac{k}{\gamma k_f}A^\gamma\right) + D_k J_{\nu/\gamma}\left(\frac{k}{\gamma k_f}A^\gamma\right)\right] \tag{4.9}$$

where $J_\alpha(z)$ is the Bessel function of order α, and ν and γ are given by

$$\nu = \frac{3}{4}(1-w_\phi) \quad ; \quad \gamma = \frac{1}{2}(1+3w_\phi) \tag{4.10}$$

We can then find $\frac{d\chi_k^{RH}}{dA}$ as follows

$$\frac{d\chi_k^{RH}}{dA} = \frac{k}{k_f}A^{-1+\gamma-\nu}\left[C_k J_{-(\nu/\gamma)-1}\left(\frac{k}{\gamma k_f}A^\gamma\right) + D_k J_{(\nu/\gamma)+1}\left(\frac{k}{\gamma k_f}A^\gamma\right)\right] \tag{4.11}$$

The coefficients C_k and D_k can be determined from the initial conditions for χ_k and $d\chi_k/dA$ at the end of inflation. It can be shown [69]

$$C_k = \frac{\pi k}{2\gamma k_f}\left[\frac{1}{1-i\left(\frac{k}{k_f}\right)}\right]\left[\frac{k}{k_f}J_{\nu/\gamma}\left(\frac{k}{\gamma k_f}\right) - \left(1-\frac{ik}{k_f}\right)J_{\nu/\gamma+1}\left(\frac{k}{\gamma k_f}\right)\right]\text{cosec}\left(\frac{\pi\nu}{\gamma}\right) \tag{4.12}$$

$$D_k = -\frac{\pi k}{2\gamma k_f}\left[\frac{1}{1-i\left(\frac{k}{k_f}\right)}\right]\left[\frac{k}{k_f}J_{-\nu/\gamma}\left(\frac{k}{\gamma k_f}\right) + \left(1-\frac{ik}{k_f}\right)J_{-(\nu/\gamma)+1}\left(\frac{k}{\gamma k_f}\right)\right]\text{cosec}\left(\frac{\pi\nu}{\gamma}\right) \tag{4.13}$$

We shall explicitly make use of the above solution and these coefficients to arrive at the present day spectrum of primary GWs.

4.1.2 Perturbative reheating

Now, we shall discuss the other reheating scenario, known as perturbative reheating (see, refs. [70], [71]). In last chapter, we discussed how the energy density of inflaton gradu-

ally decayed and transferred to radiation. In such a case, the effective EoS parameter (w_ϕ) becomes time dependent. But for simplicity, we assume it to be constant[1] during reheating.

We define two dimensionless variables which describe the comoving energy densities of inflaton and radiation

$$X(A) = \frac{\rho_\phi}{m_\phi^4} A^{3(1+w_\phi)} \quad \text{and} \quad R(A) = \frac{\rho_R}{m_R^4} A^4 \tag{4.14}$$

Now, using the conservation equation for ρ_ϕ and ρ_R [viz. Eq (3.15) and (3.20)], and writting the derivatives of ρ_ϕ and ρ_R with respect to re-scaled variable A, we can easily arrive at the Boltzmann equations governing the evolutions of energy densities [69]

$$\frac{dX}{dA} + \frac{\sqrt{3} M_{Pl} \Gamma_\phi}{m_\phi^2} (1 + w_\phi) \frac{A^{1/2} X}{\left(\frac{X}{A^{3w_\phi}} + \frac{R}{A} \right)^{1/2}} = 0 \tag{4.15}$$

$$\frac{dR}{dA} - \frac{\sqrt{3} M_{Pl} \Gamma_\phi}{m_\phi^2} (1 + w_\phi) \frac{A^{3(1-2w_\phi)/2} X}{\left(\frac{X}{A^{3w_\phi}} + \frac{R}{A} \right)^{1/2}} = 0 \tag{4.16}$$

In order to arrive at the Hubble parameter at the end of reheating, we numerically solve the above Boltzmann equations with the following initial conditions at the end of the inflation

$$\rho_\phi(A = 1) = \rho_f = 3V_f/2, \quad \rho_R(A = 1) = 0 \tag{4.17}$$

where V_f is the value of the inflationary potential at the end of the inflation. Now, it is assumed that the phase of perturbative reheating ends when the decay rate is equal to the Hubble parameter, i.e. $H = \Gamma_\phi$. So, when reheating is achieved, we require

$$H^2(A_{re}) = \frac{1}{3M_{Pl}^2} [\rho_\phi(A_{re}, n_s, \Gamma_\phi) + \rho_R(A_{re}, n_s, \Gamma_\phi))] = \Gamma_\phi^2 \tag{4.18}$$

where $A_{re} = \frac{a_{re}}{a_f}$, with a_{re} denoting the scale factor at the end of reheating and n_s is the scalar spectral index, as defined in the 2nd chapter. The end of reheating indicates to an epoch when the rate of transfer of the energy from the inflaton to radiation is maximum. Now, from the energy density of radiation ρ_R, we can determine the associated reheating temperature T_{re}, which is [72]

$$T_{re} = \left(\frac{30}{\pi^2 \, g_{r,re}} \right)^{1/4} \rho_R^{1/4}(A_{re}, n_s, \Gamma_\phi) \tag{4.19}$$

[1]This assumption is valid only when the oscillation time scale of inflaton is much smaller than the Hubble time scale.

where $g_{r,re}$ is the number of relativistic degrees of freedom associated with the reheating. We shall see later, that in order to arrive at the spectrum of GWs today, we need to fix these parameters also along with the parameters describing the inflationary potential. We shall fix the value of T_{re}, and hence determine the value of decay constant Γ_ϕ considering the condition $H = \Gamma_\phi$ at the end of reheating.

4.2 Evolution during radiation domination

In this scetion, we shall discuss the evolution of the tensor transfer function during radiation dominated epoch and arrive at the present day spectrum of primary GWs. In terms of the re-scaled scale factors, the evolution of the Hubble parameter during the radiation dominated epoch can be written as

$$H^2 = H_{re}^2 \frac{A_{re}^4}{A^4} \tag{4.20}$$

where H_{re} and A_{re} denote the Hubble parameter and re-scaled scale factor at the end of reheating, respectively. We can easily obtain the evolution equation transfer function during the radiation dominated epoch, viz. Eq[4.3]

$$\frac{d^2\chi_k}{dA^2} + \frac{2}{A}\frac{d\chi_k}{dA} + \frac{(k/k_{re})^2}{(A_{re})^2}\chi_k = 0 \tag{4.21}$$

where $k_{re} = a_{re}H_{re}$ is the mode which reenters the Hubble radius at the end of the reheating. By solving the above differential equation, we can obtain the general solution

$$\chi_k^{RD} = \frac{1}{A}\left[E_k e^{-i(k/k_{re})\left(\frac{A}{A_{re}}-1\right)} + F_k e^{i(k/k_{re})\left(\frac{A}{A_{re}}-1\right)}\right] \tag{4.22}$$

We can then match this solution and its derivative with the solution χ_k^{RH} and its derivative [viz. Eq (4.9) and (4.11)] at the end of the inflation (i.e. A=1) to determine the coefficients E_k and F_k, which can be expressed as

$$E_k = \frac{A_{re}}{2}\left[\left(1 + \frac{1k_{re}}{k}\right)\chi_k^{RH}(A_{re}) + \frac{ik_{re}}{k}A_{re}\frac{d\chi_k^{RH}}{dA}(A_{re})\right] \tag{4.23}$$

$$F_k = \frac{A_{re}}{2}\left[\left(1 - \frac{1k_{re}}{k}\right)\chi_k^{RH}(A_{re}) - \frac{ik_{re}}{k}A_{re}\frac{d\chi_k^{RH}}{dA}(A_{re})\right] \tag{4.24}$$

We can see that E_k and F_k are functions of χ_k^{RH} and $\frac{d\chi_k^{RH}}{dA}$ and thus depend on the dynamics of reheating and will be different for two reheating scenarios accordingly.

Now, considering the evolution of tensor perturbations post inflation ($h_k = h_k^P \chi_k$), we can arrive at the energy density of GWs ($\rho_{GW}(k,\eta)$), which is given by [cf. Eq(2.108)]

$$\rho_{GW}(k,\eta) = \frac{M_{Pl}^2}{2a^2}\frac{k^3}{2\pi^2}|h_k^P|^2\left(|\chi_k^{RD\,\prime}(\eta)|^2 + k^2\,|\chi_k^{RD}(\eta)|^2\right)$$

$$\implies \rho_{GW}(k,\eta) = \frac{M_{Pl}^2}{8a^2}\mathcal{P}_T(k)\left(|\chi_k^{RD\,\prime}(\eta)|^2 + k^2\,|\chi_k^{RD}(\eta)|^2\right) \tag{4.25}$$

If we now substitute the solution χ_k^{RD} [Eq (4.22)] in the above expression, we obtain $\rho_{GW}(k,\eta)$ to be

$$\begin{aligned}\rho_{GW}(k,\eta) = \frac{M_{Pl}^2 k^2}{8a_f^2 A^4}\mathcal{P}_T(k)\Bigg\{&(|E_k|^2+|F_k|^2)\left[2+\left(\frac{k_{re}A_{re}}{kA}\right)^2\right]\\ &+E_kF_k^*\left[\left(\frac{k_{re}A_{re}}{kA}\right)^2\left(1+\frac{2ik}{k_{re}}\frac{A}{A_{re}}\right)\right]e^{-2i\frac{k}{k_{re}}\left[\frac{A}{A_{re}}-1\right]}\\ &+E_k^*F_k\left[\left(\frac{k_{re}A_{re}}{kA}\right)^2\left(1-\frac{2ik}{k_{re}}\frac{A}{A_{re}}\right)\right]e^{2i\frac{k}{k_{re}}\left[\frac{A}{A_{re}}-1\right]}\Bigg\}\end{aligned} \tag{4.26}$$

We shall then be interested in the modes which re-enter the Hubble radius during reheating or radiation dominated epochs. So, during radiation domination, i.e. $A \gg A_{re}$, the above expression for ρ_{GW} simplifies to

$$\rho_{GW}(k,\eta) = \frac{M_{Pl}^2 k^2}{4a_f^2 A^4}\,\mathcal{P}_T(k)\,(|E_k|^2+|F_k|^2) \tag{4.27}$$

Hence, the dimensionless energy density of GWs (viz. Eq (2.109)) takes the form

$$\Omega_{GW}(k,\eta) = \frac{k^2}{12a_f^2H^2A^4}\,\mathcal{P}_T(k)\,(|E_k|^2+|F_k|^2) \tag{4.28}$$

We shall now introduce two new quantities [69] $\mathcal{E}_k$ and $\mathcal{F}_k$, and write them in terms of E_k and F_k respectively.

$$\begin{aligned}\mathcal{E}_k &= -i\frac{2}{A_{re}}\frac{k}{k_{re}}E_k\\ \mathcal{F}_k &= i\frac{2}{A_{re}}\frac{k}{k_{re}}F_k\end{aligned} \tag{4.29}$$

In terms of these new quantities, we can write $\Omega_{GW}(k,\eta)$ as

$$\Omega_{GW}(k,\eta) = \frac{k_{re}^2A_{re}^2}{48\,a_f^2H^2A^4}\,\mathcal{P}_T(k)\,(|\mathcal{E}_k|^2+|\mathcal{F}_k|^2) \tag{4.30}$$

Upon using equation (4.20), $k_{re} = a_{re}H_{re}$ and $A_{re} = a_{re}/a_f$ in the above equation, we obtain

$$\Omega_{GW}(k,\eta) = \frac{\mathcal{P}_T(k)}{48}\left(|\mathcal{E}_k|^2 + |\mathcal{F}_k|^2\right) \tag{4.31}$$

In case of instantaneous reheating, we have $A_{re} = 1$ and $k_{re} = k_f$. If we recall the initial conditions (see Eq.[4.4,4.5]), then we have

$$\chi_k^{RH}(A_{re}=1) = 1 \quad \text{and} \quad \frac{d\chi_k^{RH}(A_{re}=1)}{dA} = -\frac{(k/k_f)^2}{1 - i\left(\frac{k}{k_f}\right)} \tag{4.32}$$

Substituting these in Eq (4.23) and (4.24) and writing in terms of $\mathcal{E}_k$ and $\mathcal{F}_k$, we get

$$\mathcal{E}_k = \frac{1 - 2i(k/k_f) - 2(k/k_f)^2}{1 - i(k/k_f)}; \quad \mathcal{F}_k = \frac{1}{1 - i(k/k_f)} \tag{4.33}$$

As we discussed earlier that we are interested in the limit $k \ll k_f$. In this limit, $\mathcal{E}_k = \mathcal{F}_k \simeq 1$, which lead to

$$\Omega_{GW}(k,\eta) = \frac{\mathcal{P}_T(k)}{24} = \frac{H_I^2}{12\pi^2 M_{Pl}^2} \tag{4.34}$$

where we have used the scale-invariant form of tensor power spectrum [viz. Eq (2.103)].

We can see that energy density of primary GWs behaves similarly as the energy density of radiation (i.e. $1/a^4$). This is due to the fact that modes of our interest are well inside the horizon at late times during radiation domination. Finally, we can express the dimensionless energy density of primary GWs today in terms of present day dimensionless energy density of radiation as

$$\Omega_{GW}(k)h^2 \simeq \left(\frac{g_{r,0}}{g_{r,eq}}\right)\Omega_R h^2 \Omega_{GW}(k,\eta) \tag{4.35}$$

where $g_{r,eq}$ and $g_{r,0}$ represent the number of relativistic degrees of freedom at the epoch of radiation-matter equality and today, respectively. The Hubble parameter today can be expressed as $H_0 = 100h$ km s^{-1} Mpc^{-1}

4.3 Spectrum of primary GWs in instantaneous reheating

In this section, we shall discuss the exact effect of the averaged EoS on the spectrum of GWs today by choosing appropriate initial conditions in the two domains $k < k_{re}$ and $k > k_{re}$.

We can write equation (4.23) and (4.24) in terms of quantities $\mathcal{E}_k$ and $\mathcal{F}_k$ as

$$\begin{aligned}\mathcal{E}_k &= \left[\left(1-\frac{ik}{k_{re}}\right)\chi_k^{RH}(A_{re}) + A_{re}\frac{d\chi_k^{RH}}{dA}(A_{re})\right] \\ \mathcal{F}_k &= \left[\left(1+\frac{ik}{k_{re}}\right)\chi_k^{RH}(A_{re}) + A_{re}\frac{d\chi_k^{RH}}{dA}(A_{re})\right]\end{aligned} \tag{4.36}$$

Now, during radiation domination, we have $H^2A^4 = H_{re}^2A_{re}^4$ and upon using $k_f = a_fH_I$, $k_{re} = a_{re}H_{re}$, and $A_{re} = a_{re}/a_f$, we can easily obtain the following relation

$$A_{re} = \left(\frac{k_f}{k_{re}}\right)^{1/\gamma} \tag{4.37}$$

If we put this in equation (4.9), i.e in $\chi_k^{RH}(A_{re})$ solution , we get

$$\chi_k^{RH}(A_{re}) = A_{re}^{-\nu}\left[C_kJ_{-\nu/\gamma}\left(\frac{k}{\gamma k_{re}}\right) + D_kJ_{\nu/\gamma}\left(\frac{k}{\gamma k_{re}}\right)\right] \tag{4.38}$$

From the above equation, it is clear that the Bessel functions depends on (k/k_{re}) whereas C_k and D_k depend only on (k/k_f). Now, for small z ($z \ll 1$), Bessel function $J_\alpha(z)$ behaves as [73]

$$J_\alpha(z) \simeq \frac{1}{\Gamma(1+\alpha)}\left(\frac{z}{2}\right)^\alpha \tag{4.39}$$

As w_ϕ ranges from $0 \leq w_\phi \leq 1$, the quantities ν and γ both are positive.

$$\begin{aligned}J_{\nu/\gamma}(z) &\propto z^{\nu/\gamma} \quad \text{Dominant} \\ J_{-\nu/\gamma}(z) &\propto z^{-\nu/\gamma} \quad \text{Sub-dominant}\end{aligned} \tag{4.40}$$

So, we can write

$$\chi_k^{RH}(A_{re}) \simeq A_{re}^{-\nu}D_kJ_{\nu/\gamma}\left(\frac{k}{\gamma k_{re}}\right) \tag{4.41}$$

where the coefficient D_k is given by

$$D_k \simeq -\frac{\pi}{\Gamma\left(-\frac{\nu}{\gamma}\right)}\left(\frac{k}{2\gamma k_f}\right)^{-\nu/\gamma}\text{cosec}\left(\frac{\pi\nu}{\gamma}\right) \tag{4.42}$$

1. First domain ($k \ll k_{re}$): Using expression (4.39) for the Bessel function $J_{\nu/\gamma}\left(\frac{k}{\gamma k_{re}}\right)$, we can reqrite the solution $\chi_k^{RH}(A_{re})$ as

$$\chi_k^{RH}(A_{re}) \simeq -A_{re}^{-\nu}\frac{\pi}{\Gamma\left(-\frac{\nu}{\gamma}\right)}\frac{1}{\Gamma\left(1+\frac{\nu}{\gamma}\right)}\left(\frac{k}{2\gamma k_f}\right)^{-\nu/\gamma}\left(\frac{k}{2\gamma k_{re}}\right)^{\nu/\gamma}\text{cosec}\left(\frac{\pi\nu}{\gamma}\right) \tag{4.43}$$

Now using the property of the gamma function,

$$\Gamma(z)\Gamma(1-z) = \frac{\pi}{\sin(\pi z)} \tag{4.44}$$

we obtain that $\chi_k^{RH}(A_{re}) \simeq 1$ and $\frac{d\chi_k^{RH}}{dA}(A_{re}) \simeq 0$. We can also find that, under the condition $k \ll k_{re}$, we get $\mathcal{E}_k = \mathcal{F}_k \simeq 1$. So, we get the spectrum of GWs today in this domain as

$$\Omega_{GW}(k)h^2 \simeq \left(\frac{g_{r,0}}{g_{r,eq}}\right)\Omega_R h^2 \frac{\mathcal{P}_T(k)}{24} \simeq \Omega_R h^2 \frac{H_I^2}{12\pi^2 M_{Pl}^2} \tag{4.45}$$

2. Second domain ($k \gg k_{re}$): Since we are interested all the time in $k \ll k_f$ limit, D_k continues to dominate. So we can write the same previous expression for $\chi_k^{RH}(A_{re})$. Now for large argument ($z \gg 1$), the Bessel function behaves as [73]

$$J_\alpha(z) \simeq \sqrt{\frac{2}{\pi z}}\cos\left[z - (\pi\alpha/2) - \frac{\pi}{4})\right] \tag{4.46}$$

Therefore, $\chi_k^{RH}(A_{re})$ and $\frac{d\chi_k^{RH}(A_{re})}{dA}$ behave as [see Appendix (B)]

$$\chi_k^{RH}(A_{re}) \simeq \frac{1}{\sqrt{\pi}}\left(\frac{k}{2\gamma k_{re}}\right)^{-(\nu/\gamma)-(1/2)}\Gamma\left(1+\frac{\nu}{\gamma}\right)\cos\left(\frac{k}{\gamma k_{re}} - \frac{\pi\nu}{2\gamma} - \frac{\pi}{4}\right) \tag{4.47}$$

$$A_{re}\frac{d\chi_k^{RH}(A_{re})}{dA} \simeq -\frac{2\gamma}{\sqrt{\pi}}\left(\frac{k}{2\gamma k_{re}}\right)^{-(\nu/\gamma)+(1/2)}\Gamma\left(1+\frac{\nu}{\gamma}\right)\sin\left(\frac{k}{\gamma k_{re}} - \frac{\pi\nu}{2\gamma} - \frac{\pi}{4}\right) \tag{4.48}$$

Putting these two equations in equation (4.36), we get

$$\mathcal{E}_k \simeq \mathcal{F}_k^* \simeq -\frac{2i\gamma}{\sqrt{\pi}}\left(\frac{k}{2\gamma k_{re}}\right)^{-(\nu/\gamma)+(1/2)}\Gamma\left(1+\frac{\nu}{\gamma}\right)\exp i\left(\frac{k}{\gamma k_{re}} - \frac{\pi\nu}{2\gamma} - \frac{\pi}{4}\right) \tag{4.49}$$

so that,

$$|\mathcal{E}_k|^2 = |\mathcal{F}_k|^2 = \frac{4\gamma^2}{\pi}\Gamma^2\left(1+\frac{\nu}{\gamma}\right)\left(\frac{k}{2\gamma k_{re}}\right)^{n_{GW}} \tag{4.50}$$

where

$$n_{GW} = 1 - \frac{2\nu}{\gamma} = -\frac{2(1-3w_\phi)}{1+3w_\phi} \tag{4.51}$$

Therefore, we obtain

$$\Omega_{GW}(k,\eta) = \frac{\mathcal{P}_T(k)}{48}\left(|\mathcal{E}_k|^2 + |\mathcal{F}_k|^2\right) \simeq \frac{\mathcal{P}_T(k)}{24}|\mathcal{E}_k|^2 \tag{4.52}$$

If we substitute these in equation (4.35), we obtain the present day spectrum of GWs in the $k \gg k_{re}$ limit as follows:

$$\Omega_{GW}(k) \simeq \Omega_R h^2 \frac{H_I^2}{12\pi^2 M_{Pl}^2}\frac{4\gamma^2}{\pi}\Gamma^2\left(1+\frac{\nu}{\gamma}\right)\left(\frac{k}{2\gamma k_{re}}\right)^{n_{GW}} \tag{4.53}$$

where n_{GW} is the spectral index of GWs today which is given by the equation (4.51).

Chapter 5

Results and comparison with observations

In the last chapter, we have arrived at the analytical expression for the present day spectrum of GWs. Now to illustrate the results obtained in the previous chapter, we shall consider a typical inflationary model in this chapter and plot those results obtained in the last chapter. Finally we compare these with the ongoing and forthcoming GWs observations.

5.1 A typical inflationary model

In this section, we shall consider a typical inflationary model which, of course, permits the slow-roll inflation. If ϕ is the canonical scalar field (inflaton) which drives inflation, then the inflationary potential is given by

$$V(\phi) = \Lambda_0^4 \left[1 - \exp\left(-\sqrt{\frac{2}{3\alpha}}\frac{\phi}{M_{Pl}}\right)\right]^{2n} \tag{5.1}$$

This is known as $\alpha-$ attractor model of inflation. The scale Λ_0 determines the energy scale of inflation which can be constrained by observations of CMB anisotropy. We can express Λ_0 in terms of the amplitude of scalar power spectrum $\mathcal{A}_S$, n_S and r as follows:

$$\Lambda_0 = M_{Pl}\left(\frac{3\pi^2 r\mathcal{A}_s}{2}\right)^{1/2}\left[\frac{2n(2n+1)+\sqrt{4n^2+6\alpha(1+n)(1-n_S)}}{4n(1+n)}\right]^{n/2} \tag{5.2}$$

We can use the constraints on the inflationary parameters $\mathcal{A}_s$, n_S and r from Planck [37],and, using the above relation, we can suitable choose a set of values for the parameters describing the potential which are consistent with the CMB observations.

This model accounts for a large number of inflationary potentials []. We should mention that, this model with $\alpha = 1$ and $n = 1$ reduces to the well-known Higgs-Starobinsky

model of inflation [74]. Our potential contains a plateau region at suitably large values of the field, which is indeed compatible with the CMB data [37].

As we saw in the previous chapter that to evolve the background beyond inflation, we need the value of the energy density of inflaton at the end of the inflation (recall Eq [4.17]), which can be expressed in terms of the value of the potential at the end of the inflation, i.e. ($\rho_f = \frac{3}{2}V_f$). We can easily obtain V_f for our potential as

$$V_f = V(\phi_f) = \Lambda^4 \left(\frac{2n}{2n+\sqrt{3\alpha}}\right)^{2n} \tag{5.3}$$

For our discussions hereafter, we shall choose $\alpha = 1$.

5.2 Evolution of Hubble parameter and transfer function

In this section, we numerically solve the differential equation [Eq (4.15) and (4.16)] governing the evolution of inflaton and radiation energy densities, that we obtained in the last chapter. Using these solutions on equation (4.18), we have plotted (see Figure 5.1) the Hubble parameter as a function of A on log scales over the domain $1 \leq A \leq A_{re}$. We have also solved the evolution equation of tensor transfer function numerically in the case of perturbative reheating and plotted it as function of A (see figure 5.2) over the same domain. In plotting these quantities, we have set $w_\phi = 0$ and set the reheating temperature $T_{re} = 10^3$ GeV.

Taking log on both side of the equation $H^2 = H_I^2 A^{-3(1+w_\phi)}$, we can find that

$$\log H = \log H_I - (3/2)\log A \tag{5.4}$$

So the slope of the graph $\log H$ vs $\log A$ is $(-\frac{3}{2})$. We can see the slope of straight line describing $H(A)$ on Figure 5.1 is indeed $(-\frac{3}{2})$ which is compatible with $w_\phi = 0$. We can also see that the slope changes when A approaches A_{re}, which indicates the transition from inflaton to radiation implying the beginning of the radiation dominated epoch.

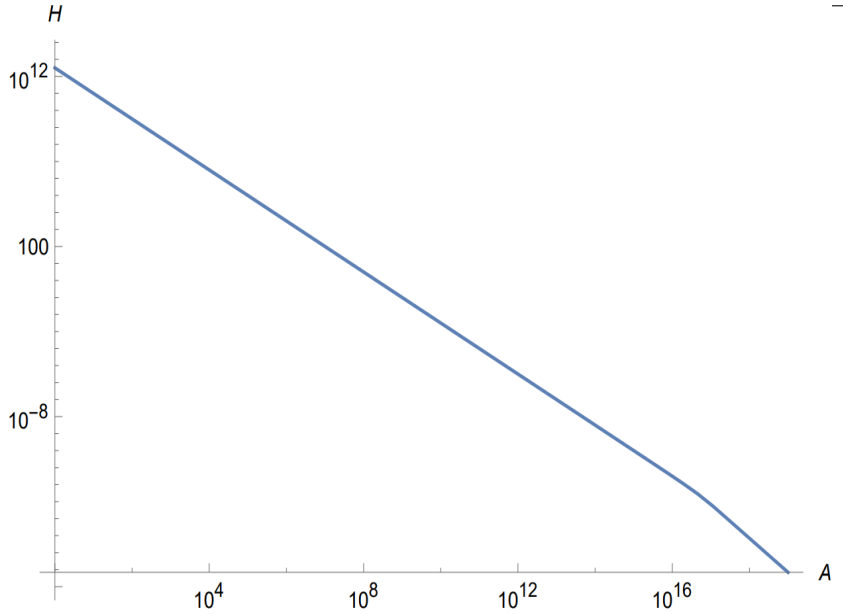

Figure 5.1: Evolution of Hubble parameter during perturbative reheating.

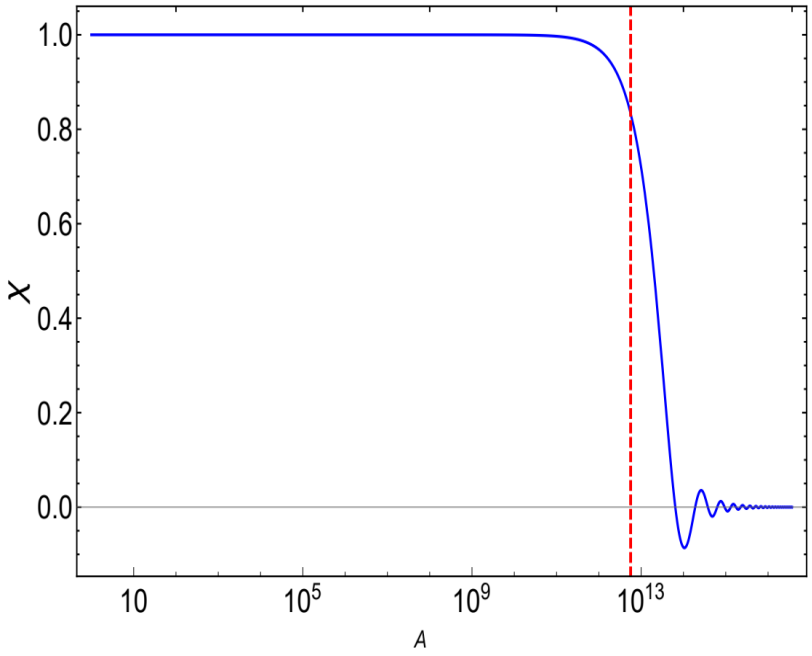

Figure 5.2: Evolution of tensor transfer function during perturbative reheating.

The vertical red line in Figure 5.2 indicates the time when the mode reenters the Hubble radius during reheating. Here we can see that transfer function is constant on super Hubble scales but it starts oscillating when the mode reenters the Hubble radius during reheating.

5.3 Spectrum of primary GWs today

In this section, we shall consider only the case of instantaneous reheating described by an averaged EoS parameter w_ϕ, to plot the spectrum of GWs today. In the previous chapter we obtained the present day spectrum of primary GWs analytically in the instantaneous reheating scenario. In the figure 5.3, we have plotted the dimensionless energy density of primary GWs today, viz. $\Omega_{GW}(f)$ over the wide range of frequencies.

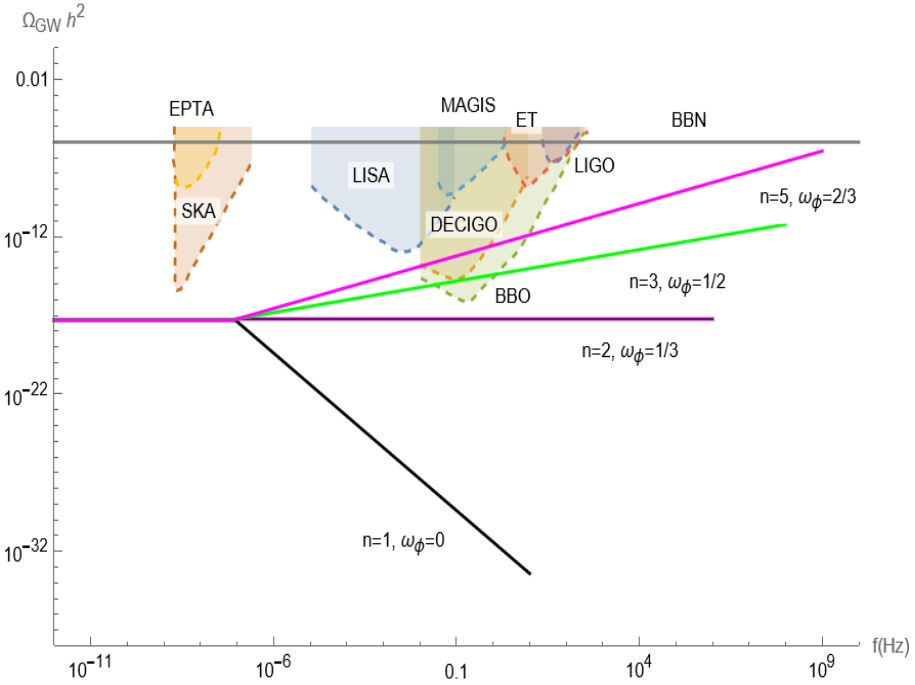

Figure 5.3: Plot of spectrum of primary GWs today, $\Omega_{GW}h^2$ as function of frequencies f on log scales.

In plotting the above spectrum, we have considered the $\alpha-$attractor model of inflation as defined in the last chapter. We have chosen a set of values for inflationary parameter n and illustrated the spectra for each n values. We have chosen $n = (1, 2, 3, 5)$, which correspond to EoS parameter $w_\phi = (0, \frac{1}{3}, \frac{1}{2}, \frac{2}{3})$. We have chosen this parameters such that $T_{re} = 3$ GeV in all the cases. If we use equation (4.51) to calculate the spectral index of GWs, i.e. $n_{GW} = -\frac{2(1-3w_\phi)}{1+3w_\phi)}$ for the set of w_ϕ values, then we get the spectral index of GWs to be $n_{GW} = (-2, 0, \frac{2}{5}, \frac{2}{3})$, as expected. As we can see, this figure illustrates the same features in the domains $k \gg k_{re}$ and $k \ll k_{re}$, as we discussed in the last chapter:
1. The spectrum of GWs is strictly scale-invariant for $f < f_{re} = \frac{k_{re}}{2\pi}$.

2. The spectrum has a red tilt for $w_\phi < \frac{1}{3}$ and a blue tilt for $w_\phi < \frac{1}{3}$ in the large frequency limit.

In the above figure, we have also included the sensitivity curves of the some of the present and proposed GW observatories. We find that for a set of values of inflationary parameter n and reheating parameter w_ϕ, the spectra of GWs intersect with the sensitivity curves of some GWs observations. Moreover, interestingly we find that the spectrum corresponding to $w_\phi = 2/3$ crosses the BBN bound of $\Omega_{GW}h^2 \leq 10^{-6}$ at large frequencies ($\sim 10^{10}$ Hz). These features of this figure suggest that observations of GWs today can prove the inflationary paradigm as well as these lead to interesting constraints on the physics of the very early universe.

5.4 Secondary epoch of reheating and spectrum of primary GWs

In the previous chapter, we had discussed the evolution of GWs during primary epoch of reheating followed by a primary radiation dominated epoch. We had also considered that the entropy conservation from reheating to today. We used that fact to relate the reheating temperature T_{re} at the end of reheating to the temperature today T_0.

Apart from these primary phases discussed earlier, there may be a short secondary phase of reheating [75] can arise after the primary radiation dominated epoch (as illustrated in Figure 5.4). This modified scenario are also compatible with observations [76], [77]. A secondary phase of reheating can occur due to the decay of another scalar field σ. This decay leads to entropy production in the universe. In this section, we shall discuss the evolution of GWs during this secondary phase of reheating. We shall see that , this secondary phase of entropy production leads to specific imprints on the present day spectrum of GWs. We shall also discuss constraints from the recent NANOGrav observation.

In order to calculate the temperature T_{re} associated with the secondary phase of reheating, we assume entropy conservation during the first radiation dominated epoch. Hence, we can find the relation between the temperature at the end of the first phase of reheating (T_{re}) and the temperature at the beginning of the secondary phase of reheating ($T_{\sigma R}$) as follows:

$$g_{s,re}\, a_{re}^3\, T_{re}^3 = g_{s,\sigma R}\, a_{\sigma R}^3\, T_{\sigma R}^3 \tag{5.5}$$

where $g_{s,re}$ and $g_{s,\sigma R}$ denote the relativistic degrees of freedom related to entropy production. Note that a_{re} and $a_{\sigma R}$ denote the scale factor at the end of primary reheating phase and at the start of the second phase of reheating respectively. We can now express the original reheating temperature T_{re} in terms of the temperature $T_{\sigma R}$ at the beginning of the secondary phase of reheating. Upon using the above relation, we get

$$T_{re} = \left(\frac{g_{s,\sigma R}}{g_{s,re}}\right)^{1/3} e^{N_{RD}^{(1)}} T_{\sigma R} \tag{5.6}$$

where $N_{RD}^{(1)} = ln\ (a_{\sigma R}/a_{re})$ denotes the number of e-folds during first epoch of radiation domination . Upon demanding the entropy conservation, we can similarly express the temperature at the end of the secondary phase of reheating, say, T_σ, in terms of the temperature T_0 today as

$$T_\sigma = \left(\frac{43}{11\ g_{s,\sigma}}\right)^{1/3} \left(\frac{a_0}{a_{eq}}\right) e^{N_{RD}^{(2)}} T_0 \tag{5.7}$$

where a_{eq} is the scale-factor during radiation-matter equality. The factor a_0/a_{eq} can be expressed in terms of the quantity a_0/a_k through the relation

$$\frac{a_0}{a_{eq}} = \left(\frac{a_0}{a_k}\right) e^{-[N_k + N_{re} + N_{RD}^{(1)} + N_{sre} + N_{RD}^{(2)}]} \tag{5.8}$$

where a_k denotes the scale factor when the mode with the wave number k leave the Hubble radius during inflation. N_k represents the number of e-folds from the time corresponding to a_k to the end of inflation. The quantities N_{re}, N_{sre} and $N_{RD}^{(2)}$ denote the number of e-folds during the first phase of reheating, second phase of reheating and second phase of radiation domination, respectively. Setting k to the pivot scale k_*, we can finally arrive at the expression for the primary reheating temperature T_{re} in terms of the parameters associated with the modified scenario of entropy production [69]:

$$T_{re} = \left(\frac{43}{11\ g_{s,\sigma}}\right)^{1/3} \left(\frac{a_0\ H_I}{k_*}\right) F^{-1/3}\ e^{-(N_* + N_{re})}\ T_0 \tag{5.9}$$

where F is the ratio of entropy calculated at the end and at the beginning of the secondary phase of reheating. It can be expressed as [69]

$$F = \frac{s(T_\sigma) a_\sigma^3}{s(T_{\sigma R}) a_{\sigma R}^3} \tag{5.10}$$

where $s(T)$ is the entropy at temperature T.

Considering the secondary phase of reheating described by averaged EoS w_σ, we can obtain the relation between Hubble parameter at the end and at the beginning of the secondary phase of reheating:

$$H_\sigma = \left(\frac{\gamma_1\, T_\sigma}{\gamma_2\, F^{1/3}\, T_{\sigma R}}\right)^{3(1+w_\sigma)/2} H_{\sigma R} \tag{5.11}$$

where $\gamma_1 = \left(\frac{g_{r,re}}{g_{r,\sigma R}}\right)^{1/4}$ and $\gamma_2 = \left(\frac{g_{s,re}}{g_{s,\sigma}}\right)^{1/3}$. Similarly, we can arrive at the relation between the temperature at the end and at the beginning of the secondary phase of reheating:

$$T_\sigma = \left(\frac{\gamma_1}{\gamma_2\, F^{1/3}}\right)^{\frac{3(1+w_\sigma)}{1-3w_\sigma}} \left(\frac{g_{r,\sigma R}}{g_{r,\sigma}}\right)^{\frac{1}{1-3w_\sigma}} T_{\sigma R} \tag{5.12}$$

The quantity of our interest is the factor F, which decides the extent of entropy produced at late times.

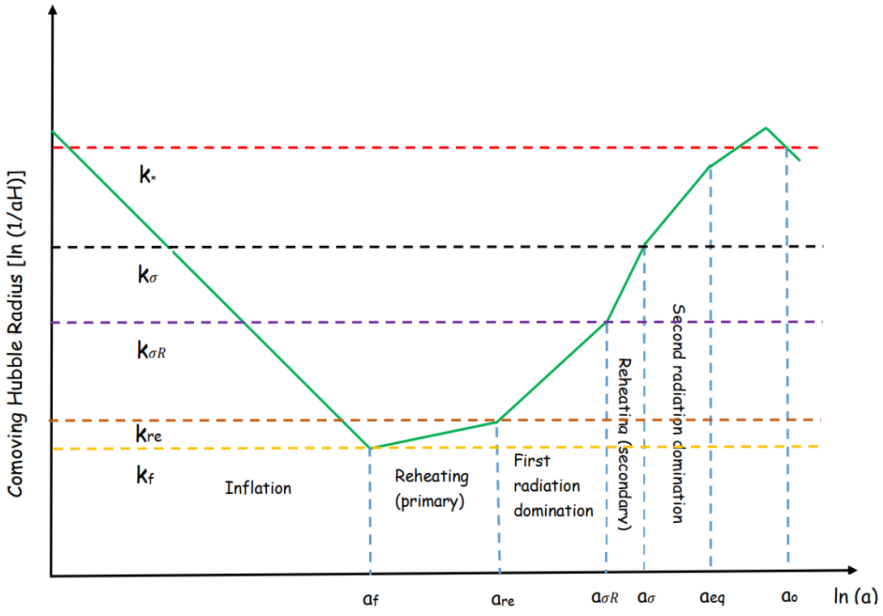

Figure 5.4: A schematic diagram describing the evolution of the Hubble radius in a scenario with a secondary reheating phase . (Fig. from [69])

In this figure, we have highlighted all the relevant scales in this modified scenario. k_* is the CMB pivot scale; $k_{\sigma R}$ and k_σ are wave numbers associated with the modes which re-enter the Hubble radius at the beginning and at the end of secondary phase of reheating respectively.

We shall now discuss the spectrum of GWs arises due to this modified scenario. Similar to the case of primary reheating, we can describe the secondary epoch of reheating by an averaged EoS parameter w_σ. In order to arrive at the present day GWs spectrum, we shall follow the same calculations as we discussed in the last chapter for the case of primary reheating. Before plotting the spectrum, we shall briefly describe the shape of the spectrum in the modified scenario.

For $\mathbf{k} < \mathbf{k}_\sigma$: These modes with wave numbers $k < k_\sigma$ re-enter the Hubble radius during the secondary radiation dominated epoch. So, prior to their re-entry, there are on super-Hubble scales which indeed implies that these modes are not affected by the dynamics of background during earlier epochs. Hence, spectrum of GWs remains scale-invariant ($n_{GW} = 0$).

For $\mathbf{k}_\sigma < \mathbf{k} < \mathbf{k}_{\sigma\mathbf{R}}$: As we have mentioned $k_{\sigma R}$ denotes the wave number which reenters the Hubble radius at the beginning of the secondary reheating phase. Similar to the case when modes re-enter the Hubble-radius during primary epoch of reheating, we expect n_{GW} to be non-zero over this range of wave numbers. The spectrum of GWs exhibits a spectral tilt and n_{GW} depends on the EoS parameter w_σ as

$$n_{GW} = \frac{2(3w_\sigma - 1)}{3w_\sigma + 1} \tag{5.13}$$

So, it is clear that the spectrum has a blue tilt when $w_\sigma > 1/3$ and a red tilt when $w_\sigma < 1/3$. Then, for these range of wave numbers, $\Omega_{GW}(k)$ behaves as

$$\Omega_{GW}(k) \propto k^{n_{GW}} \propto k^{\frac{2(3w_\sigma - 1)}{3w_\sigma + 1}} \tag{5.14}$$

For $\mathbf{k}_{\sigma\mathbf{R}} < \mathbf{k} < \mathbf{k}_{\mathbf{re}}$: These modes re-enter the Hubble radius during the first epoch of radiation domination. Thus, the spectrum of GWs should be scale invariant ($n_{GW} = 0$) over this range. The amplitude of the spectrum over this range will depend on the value of the EoS parameter w_σ, which characterizes the secondary reheating phase.

For $\mathbf{k}_{\mathbf{re}} < \mathbf{k} < \mathbf{k}_{\mathbf{f}}$: This corresponds to the case that we had discussed in the previous chapter where the corresponding modes re-enter the Hubble radius during the primary phase of reheating. So, the spectrum of GWs will behave as

$$\Omega_{GW}(k) \propto k^{n_{GW}} \propto k^{\frac{2(3w_\phi - 1)}{3w_\phi + 1}} \tag{5.15}$$

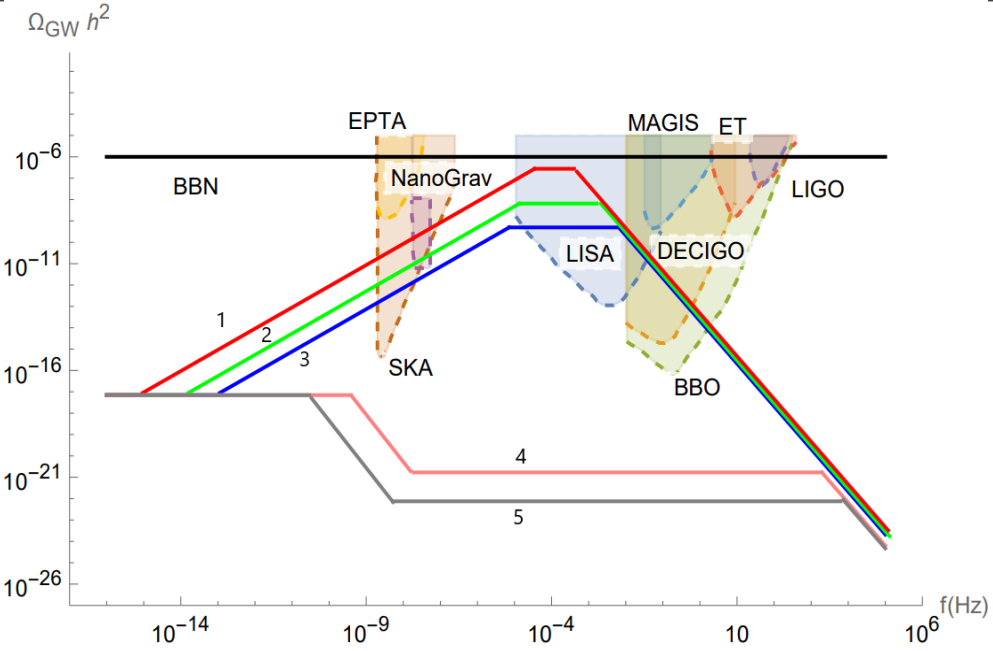

Figure 5.5: Plot of present day spectrum of primary GWs, $\Omega_{GW}(f)$ in the modified scenario with a secondary epoch of reheating.

1. $T_{re} = 10$ GeV, $F = 10^{-8}, w_\sigma = 0.99$; 3. $T_{re} = 10^3$ GeV, $F = 10^{-6}, w_\sigma = 0.99$;
2. $T_{re} = 10^2$ GeV, $F = 10^{-7}, w_\sigma = 0.99$; 4. $T_{re} = 10^{11}$ GeV, $F = 10^2, w_\sigma = 0$;
5. $T_{re} = 10^{12}$ GeV, $F = 10^3, w_\sigma = 0$.

From the above figure, we can see the effects on $\Omega_{GW}(f)$ over the frequency range $f < f_{re}$ due to the late time entropy production. I have plotted the spectra by appropriately choosing reheating temperature T_{re}, F and EoS parameter w_σ. We have also set scalar spectral index $n_S = 0.9624$ and $T_{\sigma R} = 1$ GeV. Now, recent NANOGrav observations suggest a stochastic GWs background with an amplitude of $\Omega_{GW}h^2 \simeq 10^{-11}$ around the frequency of 10^{-8} Hz [31] which lies in the domain $f < f_{re}$. It is also important to recognize the fact that, to be compatible with the NANOGrav observations, the reheating temperature T_{re} has to be less than 10^3 GeV in the modified scenario with late time entropy production. It implies a low decay width for the inflaton. Apart from the constraints from NANOGrav, we can see from figure 5.5 that the primary spectrum in the modified scenario can also be detected by some proposed future GW observatories such as DECIGO, BBO, SKA and LISA.

Chapter 6

Generation of secondary GWs

Till now, we have discussed the generation of GWs from first order tensor perturbations, and their evolution and present day spectrum. As we mentioned earlier, these are known as primary gravitational waves. Now at the second order in perturbation theory, the tensor perturbations are sourced by first order scalar perturbations ([78], [79]). These secondary tensor modes can generate secondary GWs. It is numerically studied that the present day spectrum of secondary GWs (on small scales) is accessible to proposed GWs observations like the Big Bang Observer (BBO) [6]. Recent studies show that inflationary potentials with inflection points can lead to a phase of ultra-slow-roll (for a detailed discussion, see for instance [80]), which indeed leads to the enhancement of the primordial curvature perturbations on small scales. This rise in the scalar power spectrum on small scales leads to the formation of primordial black holes (PBHs) as well as the secondary GWs with detectable amplitudes [81]. In this chapter, we shall discuss the generation mechanism and calculate the spectrum of secondary GWs induced by scalar perturbations at second order.

6.1 Second order tensors from first order scalars

In chapter 2, we had discussed the fact that the scalar, vector and tensor modes evolve independently in the first-order perturbation theory. But, at the second-order, scalar, vector and tensor modes are not independent. Interestingly, at the second order, secondary tensor modes $\tilde{h}_{ij}$ depends on the first-order scalar metric perturbation. We are interested in these scalar-induced tensor perturbations. To compute the second order tesnor modes, we begin

with the perturbed metric

$$ds^2 = a^2(\eta)\left[-\left(1+2\Phi^{(1)}+2\Phi^{(2)}\right)d\eta^2 + 2V_i^{(2)}d\eta dx^i + \left\{(1-2\Psi^{(1)}-2\Psi^{(2)})\delta_{ij}+\frac{1}{2}\tilde{h}_{ij}\right\}dx^i dx^j\right] \tag{6.1}$$

where Φ and Ψ are the Bardeen potentials (see section (2.4)) describing the scalar perturbations at the first order and (1) and (2) indicates the order of perturbation. The second-order Einstein tensor and energy-momentum tensor can be written as [82]

$$\begin{aligned} G_j^{(2)i} = a^{-2}\Bigg[&\frac{1}{4}\left(\tilde{h}_j^{i\,\prime\prime}+2\mathcal{H}\tilde{h}_j^{i\,\prime}-\nabla^2\tilde{h}_j^i\right)+2\Phi^{(1)}\partial^i\partial_j\Phi^{(1)}-2\Psi^{(1)}\partial^i\partial_j\Phi^{(1)}+4\Psi^{(1)}\partial^i\partial_j\Psi^{(1)} \\ &+\partial^i\Phi^{(1)}\partial_j\Phi^{(1)}-\partial^i\Phi^{(1)}\partial_j\Psi^{(1)}-\partial^i\Psi^{(1)}\partial_j\Phi^{(1)}+3\partial^i\Psi^{(1)}\partial_j\Psi^{(1)} \\ &+\left(\Phi^{(2)},\Psi^{(2)},V_i^{(2)}\text{terms}\right)+(\text{diagonal part})\,\delta_j^i \end{aligned} \tag{6.2}$$

and

$$T_j^{(2)i} = \left(\rho^{(0)}+p^{(0)}\right)v^{(1)\,i}v_j^{(1)}+p^{(0)}\Pi_j^{(2)\,i}+p^{(1)}\Pi_j^{(1)\,i}+p^{(2)}\delta_j^i \tag{6.3}$$

where ρ, p, v_i and Π are energy density, pressure, velocity and anisotropic stress, respectively. Upon acting the projection tensor $\hat{\mathcal{T}}_{ij}^{lm}$ on the spatial components of the Einstein equations, we get

$$\hat{\mathcal{T}}_{ij}^{lm}G_{lm}^{(2)} = \frac{1}{M_{Pl}^2}\hat{\mathcal{T}}_{ij}^{lm}T_{lm}^{(2)} \tag{6.4}$$

Projection tensor $\hat{\mathcal{T}}_{ij}^{lm}$ extracts the transverse, traceless part of any tensor. It also eliminates the terms involving the second-order perturbations, i.e. $\Phi^{(2)}$, $\Psi^{(2)}$, $V_i^{(2)}$, $p^{(2)}$, $\Pi_j^{(2)\,i}$. We have the first-order equations

$$p^{(1)} = c_s^2\rho^{(1)} \tag{6.5}$$

$$\rho^{(1)} = -\frac{2M_{Pl}^2}{a^2}\left[3\mathcal{H}\left(\Phi^{(1)}-\Psi^{(1)\prime}\right)+\nabla^2\Psi^{(1)}\right] \tag{6.6}$$

$$v_i^{(1)} = -\frac{2M_{Pl}^2}{a^2\left(\rho^{(0)}+p^{(0)}\right)}\,\partial_i\left(\Psi^{(1)\prime}+\mathcal{H}\Phi^{(1)}\right) \tag{6.7}$$

$$\Pi_j^{(1)i} = -\frac{M_{Pl}^2}{a^2p^{(0)}}\left(\partial^i\partial_j-\frac{1}{3}\delta_j^i\nabla^2\right)\left(\Phi^{(1)}-\Psi^{(1)}\right) \tag{6.8}$$

Using these first-order equations in (6.4) , we get the evolution equation

$$\tilde{h}_j^{i\,\prime\prime} + 2\mathcal{H}\tilde{h}_j^{i\,\prime} - \nabla^2\tilde{h}_j^i = -4\,\hat{\mathcal{T}}_{ij}^{lm}\mathcal{S}_{lm} \tag{6.9}$$

In order to arrive at the above equation, we have neglected the tensor part of $\Pi_j^{(2)i}$ and defined $\mathcal{S}_{ij}$ as

$$\begin{aligned} S_{ij} &= 2\Phi\partial^i\partial_j\Phi - 2\Psi\partial^i\partial_j\Phi + 4\Psi\partial^i\partial_j\Psi + \partial^i\Phi\partial_j\Phi - \partial^i\Phi\partial_j\Psi - \partial^i\Psi\partial_j\Phi + 3\partial^i\Psi\partial_j\Psi \\ &- \frac{4}{3(1+w)\mathcal{H}^2}\,\partial_i\left(\Psi^{'} + \mathcal{H}\Phi\right)\partial_j\left(\Psi^{'} + \mathcal{H}\Phi\right) - \frac{2c_s^2}{3w\mathcal{H}^2}\left[3\mathcal{H}(\mathcal{H}\Phi - \Psi^{'}) + \nabla^2\Psi\right]\partial_i\partial_j(\Phi - \Psi) \end{aligned} \tag{6.10}$$

where we have used $w = \frac{p^{(0)}}{\rho^{(0)}}$ and $\Phi^{(1)} \equiv \Phi;\ \Psi^{(1)} \equiv \Psi$.

Secondary tensor perturbations can also be decomposed in terms of the Fourier modes, say, $\tilde{h}_{\mathbf{k}}$ and the polarization tensor ϵ_{ij}^{λ}, as we did in the case of primary tensor perturbations (see equation (2.88)). The projection tensor can be written in terms of the polarization tensor as

$$\hat{\mathcal{T}}_{ij}^{lm}\mathcal{S}_{lm} = \int \frac{d^3\mathbf{k}}{(2\pi)^{3/2}}\,e^{i\mathbf{k}\cdot\mathbf{x}}\left[e_{ij}(\mathbf{k})e^{lm}(\mathbf{k}) + \bar{e}_{ij}(\mathbf{k})\bar{e}^{lm}(\mathbf{k})\right]\ \mathcal{S}_{lm}(\mathbf{k}) \tag{6.11}$$

where

$$\mathcal{S}_{lm}(\mathbf{k}) = \int \frac{d^3\mathbf{x}'}{(2\pi)^{3/2}}\,e^{-i\mathbf{k}\cdot\mathbf{x}'}\mathcal{S}_{lm}(\mathbf{x}') \tag{6.12}$$

One can find that the equation governing $\tilde{h}_{\mathbf{k}}$ can be written as

$$\tilde{h}_{\mathbf{k}}^{\lambda\prime\prime} + 2\mathcal{H}\tilde{h}_{\mathbf{k}}^{\lambda\prime} + k^2\ \tilde{h}_{\mathbf{k}}^{\lambda} = \mathcal{S}_{\mathbf{k}}^{\lambda} \tag{6.13}$$

We shall now assume that the anisotropic stresses are absent, i.e. $\Phi = \Psi$. Then, considering the source term $\mathcal{S}_{\mathbf{k}}^{\lambda}$ as a convolution of two first-order scalar perturbations at two different wavenumbers $\mathbf{k}$ and $\tilde{\mathbf{k}}$, we get [82]

$$\begin{aligned} &\mathcal{S}_{\mathbf{k}}^{\lambda}(\eta) = -4\,e^{lm}(\mathbf{k})\ \mathcal{S}_{lm}(\mathbf{k}) \\ &= 4\int \frac{d^3\tilde{k}}{(2\pi)^{3/2}}\,e^{\lambda}(\mathbf{k},\tilde{\mathbf{k}})\left\{2\Psi_{\mathbf{k}}(\eta)\ \Psi_{\mathbf{k}-\tilde{\mathbf{k}}}(\eta) + \frac{4}{3(1+w)\mathcal{H}^2}\left[\Psi_{\tilde{\mathbf{k}}}^{'}(\eta) + \mathcal{H}\Psi_{\tilde{\mathbf{k}}}(\eta)\right]\ \left[\Psi_{\mathbf{k}-\tilde{\mathbf{k}}}^{'}(\eta) + \mathcal{H}\Psi_{\mathbf{k}-\tilde{\mathbf{k}}}(\eta)\right]\right\} \end{aligned} \tag{6.14}$$

If we consider that the scales of our interest re-enter the Hubble radius during radiation dominated epoch, then $w = 1/3$ and $\mathcal{H} = 1/\eta$.

6.2 Spectrum of secondary GWs

In the previous section, we have arrived at the evolution equation of secondary tensor perturbations sourced by primary scalar perturbations [viz. (6.13)]. In this section, our motivation is to calculate the secondary tensor power spectrum and arrive at the spectrum of secondary GWs. During radiation dominated epoch (when scales of interest re-enter the Hubble radius), we can express the Fourier modes of Bardeen potential, $\Psi_{\mathbf{k}}$, in terms of the Fourier modes $\mathcal{R}_{\mathbf{k}}$ of curvature perturbation using the relation

$$\Psi_{\mathbf{k}}(\eta) = \frac{2}{3}\tilde{\chi}(k,\eta)\,\mathcal{R}_{\mathbf{k}} \tag{6.15}$$

where $\tilde{\chi}$ is the transfer function (it is different from χ defined in the chapter 5), which is given by

$$\tilde{\chi}(k,\eta) = \frac{9}{(k\eta)^2}\left[\frac{\sin\left(k\eta/\sqrt{3}\right)}{k\eta/\sqrt{3}} - \cos\left(k\eta/\sqrt{3}\right)\right] \tag{6.16}$$

Using the Green's function corrresponding to the tensor modes during radiation domination, we can write the in-homogeneous contribution to $\tilde{h}^{\lambda}_{\mathbf{k}}$ as

$$\tilde{h}^{\lambda}_{\mathbf{k}}(\eta) = \frac{4}{9k^2\eta}\int \frac{d^3\tilde{\mathbf{k}}}{(2\pi)^{3/2}}\, e^{\lambda}(\mathbf{k},\tilde{\mathbf{k}})\,\mathcal{R}_{\mathbf{k}}\mathcal{R}_{\mathbf{k}-\tilde{\mathbf{k}}}\left[\mathcal{I}_c\left(\frac{\tilde{k}}{k},\frac{|\mathbf{k}-\tilde{\mathbf{k}}|}{k}\right)\cos(k\eta) + \mathcal{I}_s\left(\frac{\tilde{k}}{k},\frac{|\mathbf{k}-\tilde{\mathbf{k}}|}{k}\right)\sin(k\eta)\right] \tag{6.17}$$

where thre quantities $\mathcal{I}_c(x,y)$ and $\mathcal{I}_s(x,y)$ can be obtained as (see ref. [81])

$$\mathcal{I}_c(x,y) = -\frac{27\pi}{4x^3y^3}\Theta(x+y-\sqrt{3})(x^2+y^2-3)^2 \tag{6.18}$$

$$\mathcal{I}_s(x,y) = -\frac{27\pi}{4x^3y^3}(x^2+y^2-3)\left[4xy + (x^2+y^2-3)\log\left|\frac{3-(x-y)^2}{3-(x+y)^2}\right|\right] \tag{6.19}$$

where $\Theta(z)$ is the theta function. From equation (6.17), we can see that $\tilde{h}^{\lambda}_{\mathbf{k}}$ involves product of $\mathcal{R}_{\mathbf{k}}$ and $\mathcal{R}_{\mathbf{k}-\tilde{\mathbf{k}}}$. Then, it is evident that the secondary tensor power spectrum will involve product of four such variables. Now, considering the fact that $\mathcal{R}_{\mathbf{k}}$ is a Gaussian random variable, we can express the four point functions in-terms of the two-point functions which are evidently the inflationary scalar power spectrum $\mathcal{P}_S(k)$. As a result, the secondary tensor power spectrum takes the form

$$\mathcal{P}_h(k,\eta) = \frac{4}{81k^2\eta^2}\int_0^{\infty} dx \int_{|1-x|}^{1+x} dy\, \left[\frac{4x^2-(1+x^2-y^2)^2}{4xy}\right]^2 \mathcal{P}_S(kx)\,\mathcal{P}_S(ky) \times \left[\mathcal{I}_c(x,y)\cos(k\eta) + \mathcal{I}_s(x,y)\sin(k\eta)\right]^2 \tag{6.20}$$

We can see that $\mathcal{P}_h(k,\eta)$ involves trigonometric functions. So, it is convenient to take average of $\mathcal{P}_h(k,\eta)$ over small time scales to replace the trigonometric functions by their time average and we get time averaged secondary tensor power spectrum as

$$\overline{\mathcal{P}_h(k,\eta)} = \frac{2}{81k^2\eta^2}\int_0^\infty dx \int_{|1-x|}^{1+x} dy \left[\frac{4x^2-(1+x^2-y^2)^2}{4xy}\right]^2 \mathcal{P}_S(kx)\,\mathcal{P}_S(ky) \times \left[\mathcal{I}_c^2(x,y)+\mathcal{I}_s^2(x,y)\right]^2 \quad (6.21)$$

The energy density of secondary GWs associated with a Fourier mode corresponding to the wave number k at a conformal time η is given by

$$\rho_{GW}(k,\eta) = \frac{M_{Pl}^2}{8}\left(\frac{k}{a}\right)^2 \overline{\mathcal{P}_h(k,\eta)} \quad (6.22)$$

Using the definition in equation (2.109), corresponding dimensionless energy density of secondary GWs can be written as

$$\Omega_{GW}(k,\eta) = \frac{\rho_{GW}(k,\eta)}{\rho_c(\eta)} = \frac{1}{24}\left(\frac{k}{\mathcal{H}}\right)^2 \overline{\mathcal{P}_h(k,\eta)} \quad (6.23)$$

When the modes are inside the Hubble-radius during radiation dominated epoch, energy density of GWs decay just as the energy density of radiation does. Quantity of our interest is the dimensionless energy density of secondary GWs today, which can be written in terms of $\Omega_{GW}(k,\eta)$ as

$$\Omega_{GW}(k) = \left(\frac{g_{*,k}}{g_{*,0}}\right)^{-1/3} \Omega_R\, h^2 \Omega_{GW}(k,\eta)$$

$$\Omega_{GW}(k)\, h^2 \simeq 1.38\times 10^{-5}\left(\frac{g_{*,k}}{106.75}\right)^{-1/3}\left(\frac{\Omega_R\, h^2}{4.16\times 10^{-5}}\right)\Omega_{GW}(k,\eta) \quad (6.24)$$

where $\Omega_R\ h^2$ is the dimensionless energy density of radiation today and $g_{*,0}$ is the number of relativistic degrees of freedom today.

6.3 Result and observational constraints

6.3.1 A typical inflationary model (ultra-slow-roll)

We shall consider an inflationary potential which allows the existence of inflection points that lead to an ultra-slow-roll (USR) phase. The potential is given by [81]

$$V(\phi) = V_0\left\{\tanh\left(\frac{\phi}{M_{\rm Pl}}\right) + A\sin\left[\frac{\tanh\left[\phi/(\sqrt{6}M_{\rm Pl})\right]}{f_\phi}\right]\right\}^2 \quad (6.25)$$

with the values of the parameters: $V_0/M_{\rm Pl}^4 = 2 \times 10^{-10}$, $A = 0.130383$, $f_\phi = 0.129576$, and $\phi_i = 6.1 M_{\rm Pl}$ where ϕ_i denotes the initial value of the inflaton. Upon choosing these values for the parameters, we can find that the point of inflection occurs at $\phi_0 = 1.05\ M_{\rm Pl}$.

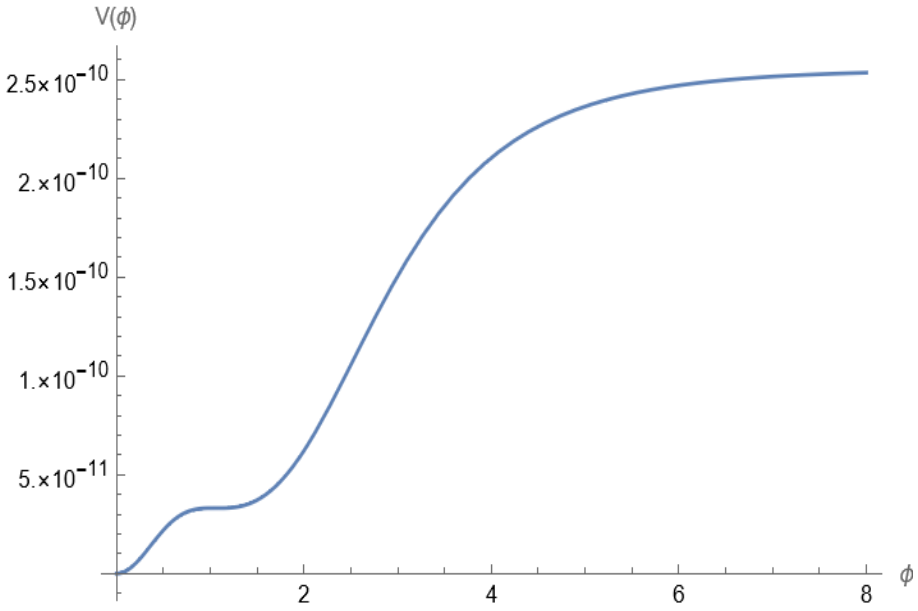

Figure 6.1: USR potential

6.3.2 Secondary GWs spectrum

We shall now plot the spectrum of secondary GWs in the USR model described by the potential (6.25). In order to do that, we numerically evaluate the scalar power spectrum for this model. We can use the expressions $\mathcal{I}_c$ and $\mathcal{I}_s$ from Eq. (6.18) and (6.19), and the scalar power spectrum together in Eq. (6.21) to get the time averaged secondary tensor power spectrum in our model. Using these in Eq. (6.24), we have plotted the dimensionless energy density of secondary GWs in Fig. (6.2). We have also added the sensitivity curves of ongoing and forthcoming GWs observations.

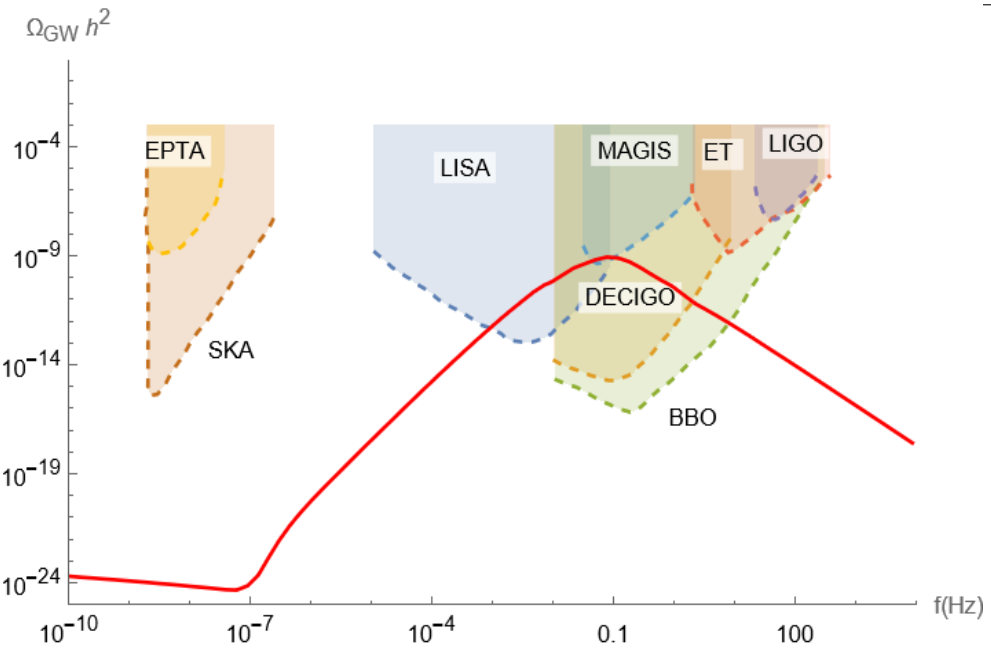

Figure 6.2: The dimensionless energy density of secondary GWs generated in USR model is plotted as function of frequency f.

From the above figure, we can see that the spectrum lies above the sensitivity curves of some future GWs observatories. It indeed suggests that we can detect the GWs generated in this USR model of inflation by some of the forthcoming GWs observatories like DECIGO, BBO and LISA.

Chapter 7

Conclusions

In this chapter, we shall briefly summarize the report and mention future implications of our work. The work that we have done and presented in this report is largely a review of the slow-roll inflation, cosmological perturbation theory and primordial gravitational waves. We have reproduced some results already available in recent literature.

We have introduced different sources and types of GWs in the first chapter. We have mentioned about a stochastic signal (relic background) of GWs from the very early universe. We have also pointed out the fact that GWs decouple immediately upon production due to the weakness of gravity and we can get a clear view of the very early universe.

In the second chapter, we have briefly discussed the successes and the drawbacks of the hot big-bang model and their solutions considering an inflationary paradigm. We have mentioned that we need scalar fields (known as inflaton) to drive inflation and briefly discussed the dynamics of inflation with particular focus on the slow-roll approximation. Then, we discussed in brief the linear cosmological perturbation theory and upon quantizing perturbations, we defined power spectra. Considering the first order tensor perturbations, and assuming de Sitter approximation, we discussed the generation of the primary GWs. Finally, we ended that chapter by defining the dimensionless energy density of GWs.

In the third chapter, we briefly described the dynamics of reheating. Considering the coupling between inflaton and radiation, we have shown how the energy density of inflaton decays exponentially and how this energy is transferred to radiation ,thus initiating a radiation-dominated epoch.

We have discussed the evolution of primary GWs through the epoch of reheating and radiation domination in chapter 4. We have mainly considered the instantaneous re-

heating scenario. We also briefly mentioned the case of perturbative reheating. Upon solving the evolution equations of tensor transfer function during instantaneous reheating and radiation-dominated epochs, we have finally obtained the spectrum of primary GWs. We have also discussed the spectrum of GWs in the modified scenario with a secondary phase of reheating.

In chapter 5, we have presented our results. Considering $\alpha-$attractor model of inflation, we have plotted the spectrum of primary GWs.
Table 1:

Wave number (k)	Index of primary GWs spectrum (n_{GW})
$k \ll k_{re}$	0
$k \gg k_{re}$	$\frac{2(3w_\phi-1)}{1+3w_\phi}$

We have shown the index of primary GWs spectrum for different range of wavenumbers in table 1. We have found that the spectrum can indeed be detected by forthcoming GWs observatories like DECIGO and BBO.
Table 2:

Wave number (k)	Index of primary GWs spectrum (n_{GW})
$k < k_\sigma$	0
$k_\sigma < k < k_{\sigma R}$	$\frac{2(3w_\sigma-1)}{1+3w_\sigma}$
$k_{\sigma R} < k < k_{re}$	0
$k_{re} < k < k_f$	$\frac{2(3w_\phi-1)}{1+3w_\phi}$

We have shown the index of primary GWs spectrum for different range of wavenumbers in table 2 in the modified scenario. We found that the strength of spectrum generated in this scenario can account for recent NANOGrav observations.

In chapter 6, we have discussed the generation of secondary GWs form the second order tensor perturbations, induced by first order scalar perturbations. We have numerically evaluated the secondary GWs spectrum in USR model of inflation. We have shown that spectrum lies above the sensitivity curves of some forthcoming GWs observatories like DECIGO, BBO and LISA which indeed reflects the possibility of detection. This study can further be extended to different inflationary models.

Appendix A

Evaluation of tensor power spectrum in slow-roll inflation

In sec. 2.3.1, we defined Hubble slow-roll parameters ϵ_H and δ_H, viz. Eq (2.50) and (2.51). Now, differentiating the conformal Hubble parameter with respect to conformal time, $\mathcal{H} = a'/a$, we get

$$\begin{aligned} \mathcal{H}' = \frac{aa'' - a'^2}{a^2} = \frac{a''}{a} - \left(\frac{a'}{a}\right)^2 \\ \Rightarrow \mathcal{H}' = \frac{a''}{a} - \mathcal{H}^2 \end{aligned} \tag{A.1}$$

From the definition of ϵ_H, we can write

$$2 - \epsilon_H = \frac{\mathcal{H}^2 + \mathcal{H}'}{\mathcal{H}^2} \tag{A.2}$$

Combining Eqs. (A.1) and (A.2), we get

$$\frac{a''}{a} = \mathcal{H}^2(2 - \epsilon_H) \tag{A.3}$$

Again, from the definition of ϵ_H,

$$\frac{1}{\epsilon_H - 1}\, d\left(\frac{1}{\mathcal{H}}\right) = d\eta \quad \text{as,} \quad \frac{d}{d\eta}\left(\frac{1}{\mathcal{H}}\right) = -\frac{\mathcal{H}'}{\mathcal{H}^2}$$

$$\Rightarrow \eta = -\int \frac{1}{1-\epsilon_H}\, d\left(\frac{1}{\mathcal{H}}\right)$$

$$\Rightarrow \eta = -\frac{1}{1-\epsilon_H}\frac{1}{\mathcal{H}} + \int \frac{d}{dN}\left(\frac{1}{1-\epsilon_H}\right)\frac{dN}{\mathcal{H}}$$

$$\Rightarrow \eta = -\frac{1}{1-\epsilon_H}\frac{1}{\mathcal{H}} + \int \frac{d\epsilon_H}{dN}\left(\frac{1}{1-\epsilon_H^2}\right)\frac{dN}{\mathcal{H}}$$

We can neglect $d\epsilon_H/dN$ term as it is quadratic in slow-roll parameters ($\ll 1$). We get,

$$\eta = -\frac{1}{1-\epsilon_H}\frac{1}{\mathcal{H}} \quad \Longrightarrow \mathcal{H} = -\left[\frac{1}{(1-\epsilon_H)\eta}\right] \tag{A.4}$$

Substituting the above equation in Eq. (A.3), we get

$$\frac{a''}{a} = \frac{1}{(1-\epsilon_H)^2\,\eta^2}(2-\epsilon_H)$$

$$\Rightarrow \frac{a''}{a} \simeq \frac{(1+2\epsilon_H)(2-\epsilon_H)}{\eta^2} \quad \text{(neglecting higher order terms in } \epsilon_H)$$

We obtain,

$$\frac{a''}{a} \simeq \frac{2+3\,\epsilon_H}{\eta^2} \tag{A.5}$$

Now recall, Mukhanov-Sasaki equation for tensor perturbations, i.e. Eq. (2.90). Substituting the above equation in Eq.(2.90), we obtain

$$u_k'' + \left[k^2 - \frac{2+3\,\epsilon_H}{\eta^2}\right] u_k = 0 \tag{A.6}$$

It can be rewritten as

$$u_k'' + \left[k^2 - \frac{\nu_T^2 - 1/4}{\eta^2}\right] u_k = 0 \tag{A.7}$$

Upon comparing Eq. (A.6) and (A.7), we find

$$\nu_T^2 = \frac{9}{4} + 3\epsilon_H$$

$$\Rightarrow \nu_T^2 \simeq (\frac{3}{2} + \epsilon_H)^2$$

$$\Rightarrow \nu_T \simeq \frac{3}{2} + \epsilon_H \tag{A.8}$$

The general solution of the Eq. (A.7) can be written as

$$u_k(k\eta) = c_1\,\sqrt{-k\eta}\,H^{(1)}_{\nu_T}(-k\eta) + c_2\,\sqrt{-k\eta}\,H^{(2)}_{\nu_T}(-k\eta) \tag{A.9}$$

where $H^{(1)}_{\nu_T}$ and $H^{(2)}_{\nu_T}$ are the Hankel functions of first and second kind. Now, imposing the Bunch-Davies initial condition, we can find

$$c_1 \simeq \frac{1}{2}\sqrt{\frac{\pi}{k}}\,e^{i(\nu_T+\frac{1}{2})\pi/2} \quad \text{and} \quad c_2 = 0 \tag{A.10}$$

So we can write the solution

$$u_k(k\eta) = \frac{1}{2}\sqrt{-\pi\,\eta}\; e^{i(\nu_T+\frac{1}{2})\pi/2}\; H^{(1)}_{\nu_T}\,(-k\eta) \tag{A.11}$$

In the super-Hubble limit ($k/aH \ll 1$), we can write the small argument limit of Hankel function:

$$H^{(1)}_{\nu_T}(x) \xrightarrow{x\to 0} \frac{1}{\Gamma(\nu_T+1)}\left(\frac{x}{2}\right)^{\nu_T} - \frac{i}{\pi}\Gamma(\nu_T)\left(\frac{2}{x}\right)^{\nu_T} \tag{A.12}$$

So, in the $k|\eta| \to 0$ limit, only second term matters and we get

$$H^{(1)}_{\nu_T}(-k\eta) \simeq -\frac{i}{\pi}\Gamma(\nu_T)\left(-\frac{2}{k\eta}\right)^{\nu_T} \tag{A.13}$$

upon using this in Eq. (A.11), we finally obtain

$$u_k(k\eta) = \frac{i}{2}\frac{1}{\sqrt{\pi k}}\; 2^{\nu_T}\; e^{i(\nu_T+\frac{1}{2})\pi/2}\;\Gamma(\nu_T)(-k\eta)^{\frac{1}{2}-\nu_T} \tag{A.14}$$

Now, substituting the above equation in the definition of tensor power spectrum, viz. Eq. (2.93), we get

$$\mathcal{P}_T(k) = \frac{4}{16\,\pi^2\,M_{\rm Pl}^2}\left(\frac{k}{a}\right)^2\left|\frac{\Gamma(\nu_T)}{\Gamma(3/2)}\right|^2\;(-k\eta)^{1-2\nu_T}\;2^{2\nu_T} \tag{A.15}$$

where we have used $\Gamma(3/2) = \sqrt{\pi}/2$. It can be further expressed in terms of the values of quantities at Hubble exit where $-k\eta = (1-\epsilon_H)^{-1}$.

$$\mathcal{P}_T(k) = \frac{2H^2}{\pi^2 M_{\rm Pl}^2}\left|\frac{\Gamma(\nu_T)}{\Gamma(3/2)}\right|^2\;2^{(2\nu_T-3)}\;(1-\epsilon_H)^{(2\nu_T-1)} \tag{A.16}$$

We can then easily see that, at the leading order in slow-roll approximation, the amplitude of tensor power spectrum takes the form

$$\mathcal{P}_T(k) \simeq \left(\frac{2H^2}{\pi^2 M_{Pl}^2}\right)_{k=aH} \tag{A.17}$$

Appendix B

Analytical derivation of the present day spectrum of primary GWs ($\Omega_{GW}(k)\ h^2$)

In chapter 4, see the solution of χ_k^{RH} from the Eq. 4.43,

$$\chi_k^{RH}(A_{re}) \simeq -A_{re}^{-\nu}\frac{\pi}{\Gamma\left(-\frac{\nu}{\gamma}\right)}\frac{1}{\Gamma\left(1+\frac{\nu}{\gamma}\right)}\left(\frac{k}{2\gamma k_f}\right)^{-\nu/\gamma}\left(\frac{k}{2\gamma k_{re}}\right)^{\nu/\gamma}\text{cosec}\left(\frac{\pi\nu}{\gamma}\right) \tag{B.1}$$

Now, we know from the property of gamma function that, $\Gamma(z)\ \Gamma(1-z) = \frac{\pi}{\sin(\pi z)}$. Usin this we can write,

$$\chi_k^{RH}(A_{re}) \simeq -A_{re}^{-\nu}\frac{\pi}{\pi/\sin\left(-\frac{\pi\nu}{\gamma}\right)}\left(\frac{k_f}{k_{re}}\right)^{\nu/\gamma}\frac{1}{\sin\left(\frac{\pi\,\nu}{\gamma}\right)}$$

$$\Rightarrow \chi_k^{RH}(A_{re}) \simeq A_{re}^{-\nu}\left(\frac{k_f}{k_{re}}\right)^{\nu/\gamma} \tag{B.2}$$

From Eq. 4.37, we have

$$A_{re}^{\nu} = \left(\frac{k_f}{k_{re}}\right)^{\nu/\gamma} \tag{B.3}$$

Thus we obtain,

$$\chi_k^{RH}(A_{re}) \simeq A_{re}^{-\nu}A_{re}^{\nu} \simeq 1 \tag{B.4}$$

So, from the above equation, we can write,

$$\frac{d\chi_k^{RH}\ (A_{re})}{dA} \simeq 0 \tag{B.5}$$

Now, under the condition, $k \ll k_{re}$, we had, $\mathcal{E}_k = \mathcal{F}_k \simeq 1$. Thus, from Eq. 4.31, we obtain

$$\Omega_{GW}(k,\eta) = \frac{\mathcal{P}_T(k)}{24} = \frac{H_I^2}{12\pi^2 M_{Pl}^2} \tag{B.6}$$

In the case of $k \gg k_{re}$, we can still write the expression

$$\chi_k^{RH}(A_{re}) \simeq A_{re}^{-\nu} D_k J_{\nu/\gamma}\left(\frac{k}{\gamma k_{re}}\right) \tag{B.7}$$

Now, in the large argument limit ($z \gg 1$),

$$J_\alpha(z) \simeq \sqrt{\frac{2}{\pi z}} \cos\left[z - (\pi\alpha/2) - \frac{\pi}{4})\right] \tag{B.8}$$

Then, we have

$$\chi_k^{RH}(A_{re}) \simeq -A_{re}^{-\nu} \frac{\pi}{\Gamma(-\nu/\gamma)} \left(\frac{k}{2\gamma\ k_f}\right)^{-\nu/\gamma} \frac{1}{\sin\left(\frac{\pi\ \nu}{\gamma}\right)} \sqrt{\frac{2\gamma\ k_{re}}{\pi k}} \cos\left[\frac{k}{\gamma\ k_{re}} - \frac{\pi\ \nu}{2\ \gamma} - \frac{\pi}{4}\right] \tag{B.9}$$

Using the property of gamma function, $\Gamma(1-z) = \frac{\pi}{\sin(\pi z)}$, we can write

$$\chi_k^{RH}(A_{re}) \simeq A_{re}^{-\nu} \left(\frac{k}{2\gamma\ k_f}\right)^{-\nu/\gamma} \Gamma\left(1+\frac{\nu}{\gamma}\right) \frac{1}{\sqrt{\pi}} \left(\frac{k}{2\ \gamma\ k_{re}}\right)^{-1/2} \cos\left[\frac{k}{\gamma\ k_{re}} - \frac{\pi\ \nu}{2\ \gamma} - \frac{\pi}{4}\right] \tag{B.10}$$

Now, using Eq. (4.37), we obtain

$$\chi_k^{RH}(A_{re}) \simeq \left(\frac{k}{2\gamma\ k_{re}}\right)^{(-\nu/\gamma\ -1/2)} \Gamma\left(1+\frac{\nu}{\gamma}\right) \frac{1}{\sqrt{\pi}} \cos\left[\frac{k}{\gamma\ k_{re}} - \frac{\pi\ \nu}{2\ \gamma} - \frac{\pi}{4})\right] \tag{B.11}$$

Then,

$$\frac{d\chi_k^{RH}\ (A_{re})}{dA} \simeq -\frac{k}{k_f}\ A_{re}^{-1+\gamma-\nu}\ D_k\ J_{\nu/\gamma\ +1}\left(\frac{k}{\gamma\ k_f}\ A_{re}^{\gamma}\right)$$

$$\Rightarrow \frac{d\chi_k^{RH}\ (A_{re})}{dA} \simeq \frac{k}{k_f}\ A_{re}^{-1+\gamma-\nu}\ \frac{\pi}{\Gamma\left(-\frac{\nu}{\gamma}\right)}\ \left(\frac{k}{2\gamma\ k_f}\right)^{-\nu/\gamma}\ \frac{1}{\sin\left(\frac{\pi\ \nu}{\gamma}\right)}\ J_{\nu/\gamma\ +1}\left(\frac{k}{\gamma\ k_{re}}\right) \tag{B.12}$$

In the limit, $k \gg k_{re}$, we can similarly express the large argument limit of the following Bessel function,

$$J_{\nu/\gamma\ +1}\left(\frac{k}{\gamma\ k_{re}}\right) \simeq \sqrt{\frac{2\ \gamma\ k_{re}}{\pi k}} \cos\left[\frac{k}{\gamma\ k_{re}} - \frac{\pi\ \nu}{2\ \gamma} - \frac{\pi}{2} - \frac{\pi}{4})\right] \tag{B.13}$$

Using this expression, we obtain,

$$\Rightarrow \frac{d\chi_k^{RH}\ (A_{re})}{dA} \simeq -\frac{k}{k_f}\ A_{re}^{(-1+\gamma-\nu)}\ \Gamma\left(1+\frac{\nu}{\gamma}\right)\ \frac{1}{\sqrt{\pi}} \left(\frac{k}{2\gamma\ k_f}\right)^{-\nu/\gamma}\ \left(\frac{k}{2\ \gamma\ k_{re}}\right)^{-1/2}$$
$$\times \cos\left[\left(\frac{k}{\gamma\ k_{re}} - \frac{\pi\ \nu}{2\ \gamma} - \frac{\pi}{4}\right) - \frac{\pi}{2})\right] \tag{B.14}$$

Thus, we can write

$$A_{re}\,\frac{d\chi_k^{RH}\,(A_{re})}{dA} \simeq -\frac{2\,\gamma}{\sqrt{\pi}}\,\Gamma\left(1+\frac{\nu}{\gamma}\right)\left(\frac{k}{2\,\gamma\,k_{re}}\right)^{-\frac{\nu}{\gamma}+\frac{1}{2}}\,\sin\left[\frac{k}{\gamma\,k_{re}}-\frac{\pi\,\nu}{2\,\gamma}-\frac{\pi}{4})\right] \tag{B.15}$$

Putting $\chi_k^{RH}(A_{re})$ and $A_{re}\,\frac{d\chi_k^{RH}\,(A_{re})}{dA}$ in Eq. (4.36) we obtain

$$\mathcal{E}_k \simeq -\frac{2i\,\gamma}{\sqrt{\pi}}\,\Gamma\left(1+\frac{\nu}{\gamma}\right)\left(\frac{k}{2\,\gamma\,k_{re}}\right)^{-\frac{\nu}{\gamma}+\frac{1}{2}}\,\left[\cos\left(\frac{k}{\gamma\,k_{re}}-\frac{\pi\,\nu}{2\,\gamma}-\frac{\pi}{4})\right)-i\,\sin\left(\frac{k}{\gamma\,k_{re}}-\frac{\pi\,\nu}{2\,\gamma}-\frac{\pi}{4})\right)\right] \tag{B.16}$$

$$\mathcal{E}_k \simeq -\frac{2i\,\gamma}{\sqrt{\pi}}\,\Gamma\left(1+\frac{\nu}{\gamma}\right)\left(\frac{k}{2\,\gamma\,k_{re}}\right)^{-\frac{\nu}{\gamma}+\frac{1}{2}}\,\exp\left[-i\left(\frac{k}{\gamma\,k_{re}}-\frac{\pi\,\nu}{2\,\gamma}-\frac{\pi}{4})\right)\right] \tag{B.17}$$

We can similarly find that, $\mathcal{E}_k \simeq \mathcal{F}_k^*$. Therefore, we get

$$|\mathcal{E}_k|^2 = |\mathcal{F}_k|^2 = \frac{4\gamma^2}{\pi}\Gamma^2\left(1+\frac{\nu}{\gamma}\right)\left(\frac{k}{2\gamma k_{re}}\right)^{n_{GW}} \tag{B.18}$$

where

$$n_{GW} = 1-\frac{2\nu}{\gamma} = -\frac{2(1-3w_\phi)}{1+3w_\phi)} \tag{B.19}$$

Therefore, we obtain

$$\Omega_{GW}(k,\eta) = \frac{\mathcal{P}_T(k)}{48}\,(|\mathcal{E}_k|^2+|\mathcal{F}_k|^2) \simeq \frac{\mathcal{P}_T(k)}{24}|\mathcal{E}_k|^2 \tag{B.20}$$

Bibliography

[1] Virgo, LIGO Scientific, B.P. Abbott et al., Phys. Rev. Lett. 116 (2016) 061102, 1602.03837

[2] R. Abbott et al., "Observation of Gravitational Waves from Two Neutron Star–Black Hole Coalescences", 2021 ApJL 915 L5, DOI: 10.3847/2041-8213/ac082e

[3] P. Abbott et al. (LIGO Scientific, Virgo), Phys. Rev. Lett. 118, 121101 (2017) [Erratum: Phys.Rev.Lett. 119, 029901 (2017)], arXiv:1612.02029 [gr-qc].

[4] M. Punturo et al. Class. Quant. Grav. 27, 194002 (2010).

[5] B. Sathyaprakash et al., Class. Quant. Grav. 29, 124013 (2012)[Erratum: Class.Quant.Grav. 30, 079501 (2013)],arXiv:1206.0331 [gr-qc].

[6] J. Crowder and N. J. Cornish, Phys. Rev. D72, 083005 (2005) arXiv:gr-qc/0506015 [gr-qc].

[7] V. Corbin and N. J. Cornish, Class. Quant. Grav. 23, 2435 (2006), arXiv:gr-qc/0512039 [gr-qc].

[8] J. Baker et al., (2019), arXiv:1907.11305 [astro-ph.IM].

[9] N. Seto, S. Kawamura, and T. Nakamura, Phys. Rev. Lett. 87, 221103 (2001), arXiv:astro-ph/0108011.

[10] S. Kawamura et al., Class. Quant. Grav. 28, 094011 (2011).

[11] S. Sato et al., J. Phys. Conf. Ser. 840, 012010 (2017).

[12] P. Amaro-Seoane et al., GW Notes 6, 4 (2013), arXiv:1201.3621 [astro-ph.CO].

[13] P. Amaro-Seoane et al. (LISA), (2017) arXiv:1702.00786 [astro-ph.IM].

[14] E. Barausse et al., (2020), 10.1007/s10714-020-02691-1., arXiv:2001.09793 [gr-qc].

[15] G. Janssen et al., PoS AASKA14, 037 (2015), arXiv:1501.00127 [astro-ph.IM].

[16] C. Moore, R. Cole, and C. Berry, "Gravitational-wave sensitivity curves" Class. Quant. Grav. 32, 015014 (2015), arXiv:1408.0740 [gr-qc].

[17] Gravitational Waves Spectrum- TAPIR (Caltech)

[18] B. Allen, 1997, January. "The stochastic gravity-wave background: sources and detection." In Relativistic Gravitation and Gravitational Radiation, Proceedings of the Les Houches School of Physics, held in Les Houches, Haute Savoie (Vol. 26, pp. 373-418). arXiv:gr-qc/9604033

[19] L.M. Krauss, S. Dodelson, and S. Meyer, 2010. Primordial gravitational waves and cosmology. Science, 328(5981), pp.989-992. arXiv:1004.2504 [astro-ph.CO]

[20] J.L. Cook and L. Sorbo, 2012. "Particle production during inflation and gravitational waves detectable by ground-based interferometers." Physical Review D, 85(2), p.023534. arXiv:1109.0022 [astro-ph.CO]

[21] Ruth Durrer, 2010 Journal of Physics: Conference Series 222 (2010) 012021. "Gravitational waves from cosmological phase transitions." doi:10.1088/1742-6596/222/1/012021.

[22] Y. Akrami et al. (Planck), Astron. Astrophys. 641, A10 (2020), arXiv:1807.06211 [astro-ph.CO].

[23] E. Aubourg et al., Phys. Rev. D 92, 123516 (2015), , arXiv:1411.1074 [astro-ph.CO].

[24] J. A. V´azquez, L. E. Padilla, and T. Matos, (2018) arXiv:astro-ph/9306029.

[25] M. S. Turner, M. J. White, and J. E. Lidsey, Phys. Rev. D 48, 4613 (1993), arXiv:astro-ph/9306029.

[26] K. Nakayama, S. Saito, Y. Suwa, and J. Yokoyama, JCAP 06, 020 (2008), arXiv:0804.1827 [astro-ph].

[27] S. Kuroyanagi, T. Takahashi, and S. Yokoyama, JCAP 02, 003 (2015), arXiv:1407.4785 [astro-ph.CO].

[28] H. Assadullahi and D. Wands, Phys. Rev. D 79, 083511 (2009), arXiv:1407.4785 [astro-ph.CO]

[29] R. Durrer and J. Hasenkamp, Phys. Rev. D 84, 064027 (2011), arXiv:1105.5283 [gr-qc].

[30] N. Bernal, A. Ghoshal, F. Hajkarim, and G. Lambiase, JCAP 11, 051 (2020), arXiv:2008.04959 [gr-qc].

[31] Z. Arzoumanian et al. (NANOGrav),Astrophys. J. Lett. 905, L34 (2020) arXiv:2009.04496 [astro-ph.HE].

[32] M. V. Sazhin, Vestn. Mosk. Univ. Fiz. Astron. 18, 82 (1977). arXiv:1612.02029 [gr-qc]

[33] S. L. Detweiler, Astrophys. J. 234, 1100 (1979). DOI: 10.1086/157593

[34] R. Brout, F. Englert and E. Gunzig, Annals Phys. 115 (1978) 78.

[35] A.A. Starobinsky, Phys. Lett. B91 (1980) 99.

[36] A.D. Linde, Phys. Lett. B108 (1982) 389.

[37] N. Aghanim et al. “Planck 2018 results. VI. Cosmological parameters”. In: Astron. Astrophys. 641 (2020), A6. DOI: 10.1051/0004-6361/201833910. arXiv: 1807.06209 [astro-ph.CO]

[38] D. J. Fixsen. “The Temperature of the Cosmic Microwave Background”. In: Astrophys. J. 707 (2009), pp. 916–920. DOI: 10 . 1088 / 0004 - 637X / 707 / 2 / 916. arXiv: 0911 . 1955[astro-ph.CO].

[39] Craig J Copi, David N. Schramm, Michael S. Turner. "Big-Bang Nucleosynthesis and the Baryon Density of the Universe." Science 267 (1995) 192-199. DOI: 10.1126/science.7809624. arXiv: astro-ph/9407006v2.

[40] Cyburt Richard, H., Fields Brian, D., Olive Keith, A. and Yeh, T.H., 2016. Big Bang Nucleosynthesis: 2015. Rev. Mod. Phys, 88, p.015004. arXiv:1505.01076v1 [astro-ph.CO].

[41] M. Colless et al., Mon. Not. Roy. Astron. Soc. 328, 1039 (2001) arXiv.astro-ph/0106498

[42] K. Abazajian et al., Astrophys. J. Suppl. 182, 543 (2009). DOI= 10.1088/0067-0049/182/2/543, arXiv:0812.0649 [astro-ph]

[43]] J. Dunkley et al., Astrophys. J. Suppl. 180, 306 (2009); E. Komatsu et al., Astrophys. J. Suppl. 180, 330 (2009); D. Larson et al., Astrophys. J. Suppl. 192, 16 (2011); E. Komatsu et al., Astrophys. J. Suppl. 192, 18 (2011); C. L. Bennett et al., Astrophys. J. Suppl. 208, 20 (2013); G. Hinshaw et al., Astrophys. J. Suppl. 208, 19 (2013). arXiv:0803.0547 [astro-ph]

[44] J. Yadav, S. Bharadwaj, B. Pandey, and T. R. Seshadri, Mon. Not. Roy. Astron. Soc. 364, 601 (2005); doi = 10.1111/j.1365-2966.2005.09578.x P. Sarkar, J. Yadav, B. Pandey and S. Bharadwaj, Mon. Not. Roy. Astron. Soc. 399, L128 (2009), arXiv ePrint: 2008.10266

[45] P.J.E. Peebles and B. Ratra, 2003. "The cosmological constant and dark energy". Reviews of modern physics, 75(2), p.559. arXiv:astro-ph/0207347

[46] S. Weinberg, Cosmology (Oxford University Press, Oxford, England, 2008). ISBN13: 978-0-19-852682-7. DOI: 10.1007/s10714-008-0728-z

[47] L. Sriramkumar. “An introduction to inflation and cosmological perturbation theory”. In: (Apr. 2009). arXiv: 0904.4584 [astro-ph.CO].

[48] D. N. Spergel et al., Astrophys. J. Suppl. 148, 175 (2003). arXiv:astro-ph/0302209

[49] A. Riotto, 2002. Inflation and the theory of cosmological perturbations. arXiv preprint hep-ph/0210162.

[50] Alan H. Guth, "The Inflationary Universe: A Possible Solution to the Horizon and Flatness Problems". Phys.Rev.D 23 (1981) 347-356, Adv.Ser.Astrophys.Cosmol. 3 (1987) 139-148 (reprint), DOI: 10.1103/PhysRevD.23.347

[51] S. Dodelson, Modern Cosmology (Academic Press, San Diego, U.S.A., 2003). ISBN 0-12-219141-2, 2003, XIII + 440 p. ui.adsabs.harvard.edu/abs/2003moco.book

[52] J.A.S. Lima, and S. Basilakos, 2011. "From de Sitter to de Sitter: A New Cosmic Scenario without Dark Energy". arXiv:1106.1938 .

[53] A.R. Liddle, P. Parsons, and J.D. Barrow, 1994. "Formalizing the slow-roll approximation in inflation". Physical Review D, 50(12), p.7222., arXiv:astro-ph/9408015

[54] V. Mukhanov. Physical Foundations of Cosmology. Oxford: Cambridge University Press, 2005. ISBN: 978-0-521-56398-7. DOI: 10.1017/CBO9780511790553

[55] L. Sriramkumar, Curr. Sci. 97, 868 (2009); L. Sriramkumar, in Vignettes in Gravitation and Cosmology, Eds. L. Sriramkumar and T. R. Seshadri (World Scientific, Singapore, 2012), pp. 207-249.

[56] E. Lifshitz, J. Phys. (USSR) 10, 116 (1946); E. M. Lifshitz and I. M. Khalatnikov, Adv. Phys. 12, 185 (1963).

[57] J. M. Bardeen, "Gauge-invariant cosmological perturbations". Phys. Rev. D 22, 1882 (1980).

[58] R.H. Brandenberger, 2004. "Lectures on the Theory of Cosmological Perturbations." In The early universe and observational cosmology (pp. 127-167). Springer, Berlin, Heidelberg. arXiv:hep-th/0306071

[59] L. P. Grishchuk, Sov. Phys. JETP 40, 409 (1974). "Amplification of gravitational waves in an istropic universe".

[60] V. S. Mukhanov, JETP Lett. 41, 493 (1985). "Cosmological Perturbations in the Inflationary Universe", DOI: 10.1016/0370-2693(87)91691-1.

[61] Misao Sasaki, "Large Scale Quantum Fluctuations in the Inflationary Universe", Progress of Theoretical Physics, Volume 76, Issue 5, November 1986, Pages 1036–1046, doi.org/10.1143/PTP.76.1036

[62] A. Kaya, 2021. "The imprint of primordial gravitational waves on the CMB intensity profile". Physics Letters B, 817, p.136353. arXiv:2105.02236 [astro-ph.CO]

[63] Planck Collaboration, A A 641, A10 (2020), [arxiv:1807 06211[astro-ph]

[64] L. A. Boyle and P. J. Steinhardt, "Probing the early universe with inflationary gravitational waves", Phys. Rev. D 77, 063504 (2008) , arXiv:astro-ph/0512014.

[65] Andrew R. Liddle, David H. Lyth, "Cosmological Inflation and Large-Scale Structure", ISBN:9781139175180, Cambridge University Press

[66] Baumann, D., 2009. TASI lectures on inflation. arXiv preprint, arXiv:0907.5424.

[67] L. Sriramkumar, "On the generation and evolution of perturbations during inflation and reheating", Vignettes in Gravitation and Cosmology, pp. 207-249 (2012)

[68] M. S. Turner and F. Wilczek, "Reheating an Inflationary Universe", Phys. Rev. Lett. 48, 1437 (1982).

[69] M.R. Haque, D. Maity, T. Paul, and L. Sriramkumar, 2021. "Decoding the phases of early and late time reheating through imprints on primordial gravitational waves". Physical Review D, 104(6), p.063513., arXiv:2105.09242 [astro-ph.CO]

[70] D. Maity and P. Saha, "Connecting CMB anisotropy and cold dark matter phenomenology via reheating" Phys. Rev. D 98, 103525 (2018) , arXiv:1801.03059 [hep-ph].

[71] M. R. Haque, D. Maity, and P. Saha, "Two phase reheating: CMB constraints on inflaton and dark matter phenomenology", Phys. Rev. D 102, 083534 (2020) , arXiv:2009.02794 [hep-th] .

[72] Edward W. Kolb, Michael S. Turner, 1990. "The Early Universe", Front.Phys. 69 (1990) 1-547, ISBN: 9780201626742

[73] I. S. Gradshteyn and I. M. Ryzhik, Table of integrals, series, and products, seventh ed. (Elsevier/Academic Press, Amsterdam, 2007) pp. xlviii+1171, translated from the Russian, Translation edited and with a preface by Alan Jeffrey and Daniel Zwillinger, With one CD-ROM (Windows, Macintosh and UNIX).

[74] A. A. Starobinsky, "A new type of isotropic cosmological models without singularity", Adv. Ser. Astrophys. Cosmol. 3, 130 (1987).

[75] M. Kawasaki and F. Takahashi, "Late-time entropy production due to the decay of domain walls". Phys. Lett. B 618, 1 (2005), arXiv:hep-ph/0410158.

[76] S. Kuroyanagi, C. Ringeval, and T. Takahashi, "Early Universe Tomography with CMB and Gravitational Waves". Phys. Rev. D 87, 083502 (2013) , arXiv:1301.1778 [astro-ph.CO].

[77] H. Hattori, T. Kobayashi, N. Omoto, and O. Seto, "Entropy production by domain wall decay in the NMSSM" Phys. Rev. D 92, 103518 (2015) , arXiv:1510.03595 [hep-ph] .

[78] K. Nakamura, "Second-order gauge invariant cosmological perturbation theory: Einstein equations in terms of gauge invariant variables," Prog. Theor. Phys. 117, 17 (2007), [arXiv:gr-qc/0605108].

[79] H. Noh and J. c. Hwang, "Second-order perturbations of the Friedmann world model," Phys. Rev. D 69, 104011 (2004), arXiv:astro-ph/0305123

[80] C.Pattison, V. Vennin, H. Assadullahi, and D. Wands, 2018. "The attractive behaviour of ultra-slow-roll inflation". Journal of Cosmology and Astroparticle Physics, 2018(08), p.048. arXiv:1806.09553 [astro-ph.CO]

[81] H.V. Ragavendra, P. Saha, L. Sriramkumar, and J. Silk, , 2021. "Primordial black holes and secondary gravitational waves from ultraslow roll and punctuated inflation." Physical Review D, 103(8), p.083510. arXiv:2008.12202 [astro-ph.CO]

[82] D. Baumann, P. Steinhardt, K. Takahashi, and K. Ichiki, 2007. "Gravitational wave spectrum induced by primordial scalar perturbations." Physical Review D, 76(8), p.084019. arXiv:hep-th/0703290